https://doi.org/10.5194/nhess-2022-112
Preprint. Discussion started: 6 April 2022


Natural Hazards and Earth System Sciences
Discussions

# Large-scale risk assessment on snow avalanche hazard in alpine regions

Gregor Ortner[1,2,3], Michael Bründl[1,2], Chahan M. Kropf[3, 4], Thomas Röösli[3,4], Yves Bühler[1,2], and David N. Bresch[3,4]

[1]WSL Institute for Snow and Avalanche Research SLF, 7260 Davos Dorf, Switzerland
[2]Climate Change, Extremes and Natural Hazards in Alpine Regions Research Center CERC, 7260 Davos Dorf, Switzerland
[3]Institute for Environmental Decisions, ETH Zurich, Universitätstr. 16, 8092 Zurich, Switzerland
[4]Federal Office of Meteorology and Climatology MeteoSwiss, Operation Center 1, P.O. Box 257, 8058 Zurich-Airport, Switzerland

**Correspondence:** Gregor Ortner (gregor.ortner@slf.ch)

**Abstract.** Snow avalanches are recurring natural hazards that affect the population and transport infrastructure in alpine regions during the winter months such as in the most recent avalanche winters of 2018 and 2019, where large damages were caused by avalanches throughout the Alps. Decision makers need detailed information on the spatial distribution of the hazard and risk in order to prioritize and apply appropriate adaptation strategies and mitigation measures to minimize impacts. Here, we present a novel risk assessment approach for assessing the spatial distribution of avalanche risk by combining large-scale hazard mapping with a state-of-the-art risk assessment tool, where risk is understood as the product of hazard, exposure, and vulnerability. Hazard disposition is modeled using the large-scale hazard indication mapping method RAMMS::LSHIM, and risks are assessed using the probabilistic Python-based risk assessment platform CLIMADA, developed at ETH Zürich. The avalanche hazard mapping for scenarios with a 30, 100, and 300 year return period is based on a high-resolution terrain model, 3-day snow depth increase, automatically determined potential release areas, and protection forest information. Avalanche hazard for 40,000 single snow avalanches is assessed in avalanche intensity measured as pressure. Exposure is represented with a detailed building layer indicating the spatial distribution of monetary assets. Vulnerability of the buildings is defined by damage functions based on the software EconoMe, which is in operational use in Switzerland. The outputs of the hazard, exposure, and vulnerability analyses are combined to quantify the risk in spatially explicit risk maps. The risk considers the probability and intensity of snow avalanche occurrence as well as the concentration of vulnerable, exposed buildings. Uncertainty and sensitivity analyses were performed to capture inherent variability in the input parameters. This new risk assessment approach allows for the quantification of avalanche risk on large scales and results in maps that show the spatial distribution of risk at specific locations. Large-scale risk maps can assist decision makers in identifying areas where hazard mitigation and/or adaption is needed to address current and future avalanche risk.

https://doi.org/10.5194/nhess-2022-112
Preprint. Discussion started: 6 April 2022


Natural Hazards and Earth System Sciences Discussions
Open Access
EGU

## 1 Introduction

In a time of densely populated alpine landscapes and continuous socio-economic growth, society is increasingly exposed to natural hazards (Zgheib et al., 2020). In mountainous regions such as the Alps, avalanches are a significant natural hazard in winter causing damage to buildings and infrastructure. In the past 20 years, alpine countries such as Switzerland have experienced multiple catastrophic avalanche situations. In winter 2019, for example, exceptional snowfall events which caused high damages throughout Switzerland (Trachsel et al., 2020). The winter 2017/18 was the first since the catastrophic avalanche winter of 1999 (Wiesinger and Adams, 2007) in which the highest avalanche danger, level 5, was forecasted for wide areas across the Swiss Alps. In January 2018, 2.5 to 5 m of snow fell at higher altitudes within 25 days. Numerous avalanches in the categories "large" and "very large" were counted (Zweifel et al., 2019). In total, over 380 avalanches caused a damage to buildings, traffic routes, or important infrastructure in Switzerland (Bründl et al., 2019), making it to the most severe avalanche winter in recent years, not only in Switzerland, but also in Austria, and Germany (MeteoSchweiz, 2019; Pancevski, 2019; ZAMG, 2020; Trachsel et al., 2020). Such events show that even in highly developed, well adapted countries, society is still vulnerable to extreme snowfall events causing avalanche hazards. Strategies, methods, and risk assessments to counteract this threat are well developed in most areas in the Alps, but they need to be continuously developed to strengthen and improve the resilience of the population and their assets (Zgheib et al., 2020).

To cope with natural hazards threatening exposed assets, the concept of risk has been introduced in Switzerland in the late 1990s to support decision makers for dealing with natural hazards (Heinimann et al., 1998; Borter, 1999; Bründl et al., 2009). The risk concept became also the central element of the Strategy for Natural Hazards of the National Platform Natural Hazards (PLANAT) in Switzerland (PLANAT, 2009, 2018). In the context of natural hazards in Switzerland, risk is defined as the product of hazard potential, objects at risk (exposure) and their vulnerability (Borter and Bart, 1999). In more detail, Bründl et al., defines risk as the damage that is statistically expected due to the hazard intensity (= caused by avalanche pressure) in a given scenario, calculated as the product of the expected damage and the frequency (= 1/return period) of this scenario. More generally, the IPCC defines risk as the likelihood for the disturbance of the normal functionality of a society due to a hazardous physical event under vulnerable social conditions (= vulnerability) with economic, material or environmental consequences (IPCC, 2014), see also Fig. 1. In this study, we use an extended definition of the IPCC risk concept by Aznar-Siguan and Bresch (2019) expressing risk as the probability of a consequence and its severity:

$$\text{risk} = \text{probability} \times \text{severity} \tag{1}$$

, where

$$\text{severity} = F(\text{hazard intensity, exposure, vulnerability}) = \text{exposure} \times f_{imp}(\text{hazard intensity}) \tag{2}$$

Overviews on natural hazards risks and vulnerabilities in different spatial scales were generated by various institutions in the last decade (MATRIX Consortium, 2013; van Westen and Greiving, 2017; Fuchs et al., 2019; FOEN, 2020). These studies vary

https://doi.org/10.5194/nhess-2022-112
Preprint. Discussion started: 6 April 2022


Natural Hazards and Earth System Sciences
Discussions

from vulnerability surveys (Fuchs et al., 2015) to multi-risk and resilience approaches (Kappes et al., 2012; Komendantova et al., 2016). Projects such as RoadRisk carried out by the Swiss Federal Roads Office (ASTRA, 2012) or the National Risk Overview initiated by the Swiss Federal Office for the Environment (FOEN, 2020) indicate the demand for large-scale risk surveys. What is missing so far, is a method to assess avalanche risk at a regional or national scale, which would allow decision-makers to identify hot spots of avalanche risk. Such hot spots show where detailed assessment would be necessary to develop appropriate adaptation measures.

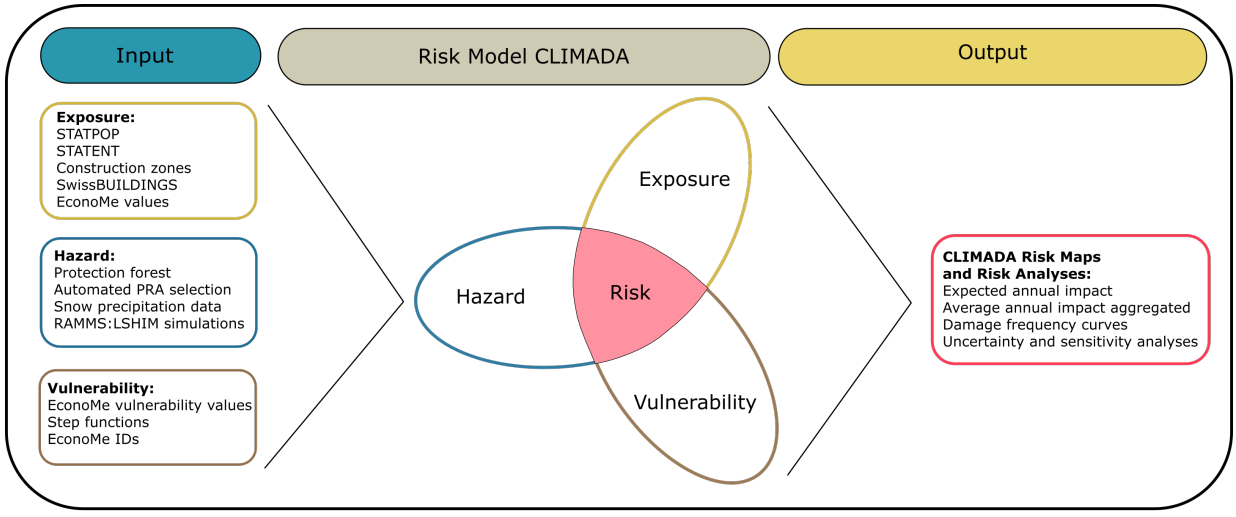


**Figure 1.** A schematic illustration of the IPCC risk concept with the used input data for generating information on exposure, hazard and vulnerability, used to create risk maps and perform risk analyses.

The goal of this study is to suggest a framework for assessing avalanche risk at a large scale, as it is presented in Fig. 1. The method was applied to a region in central Switzerland, but could be deployed anywhere in the world. Since the components of risk are not constant, such a framework can also help to depict changes of the components of risk, such as hazard, exposure and vulnerability over time and space. In this paper, we focus on the presentation of the framework for the current risk situation, which will serve as a platform for modelling expected climate and socio-economic induced changes of risk in future.

Especially in the context of climate change and population growth, new strategies and tools that assist in exposed regions to systematically identify risk and respond to threats in exposed areas are of increasing importance (IPCC, 2012). Changes in the climate system and their influence on local weather phenomena do not only affect us already (CH2018, 2018), but will likely lead to an increase of the frequency and magnitude of natural hazards in the years to come (IPCC, 2014). In particular, various studies indicate that changes in the climate system, such as temperature rise and an increase of extreme precipitation events, will likely influence gravity-driven hazards (Mani and Caduff, 2012; Ballesteros-Cánovas et al., 2018), such as snow avalanches.

https://doi.org/10.5194/nhess-2022-112
Preprint. Discussion started: 6 April 2022


Natural Hazards and Earth System Sciences Discussions

The paper is organised as follows. First, we present the method in detail followed by a section in which we show how this new method operates and how it can be applied to specific examples, such as the case study in central Switzerland. In the result section, we show the spatial distribution of the calculated risks, analyse the uncertainties and perform a sensitivity study. Finally, we discuss progress and limitations of the new method and conclude finally, how this framework might contribute to a dialogue on the changes of risk at a large scale.

## 2 Methods

Since our consideration of risk requires the three components of hazard, vulnerability and exposure (see Fig. 1), the methods chapter is organized into these subsections. These subsections contain the information on how the respective components were generated in this study and how they are used to calculate the spatially distributed risk.

### 2.1 Hazard - Avalanche hazard indication mapping with RAMMS::LSHIM

Hazard indication mapping of snow avalanches at a scale of 1:5,000 to 1:10,000 was carried out for backcountry users (Harvey et al., 2018) and exposed communities in Switzerland (Bühler et al., 2022), Italy (Maggioni et al., 2018; Monti et al., 2018), and other regions worldwide (Bühler et al., 2018). For this study we focus on the Gotthard region in central Switzerland, which is one of the most important north-south transit corridors in the alps and has a long avalanche history and is still frequently threatened by avalanches (Fig. 5) . In order to cover all possible avalanches affecting the region, every hydrological catchment stretching from the main valley up to the mountain ridges of the side valleys was regarded as potential process areas. The individual catchments were combined into a large comprehensive perimeter outlining the study area (Fig. 3). To identify relevant catchment areas that are particularly affected by avalanches, a data set of all historical damaging avalanches observed and recorded by the WSL Institute for Snow and Avalanche Research SLF and cantonal and federal authorities were taken as a basis. The combination of the hydrological catchment areas also includes areas that have no avalanche records but may still be relevant for hazard mapping.

#### 2.1.1 Creation of the avalanche protection forest layer and delineation of the release areas

Forest influences the snowpack structure by interception, micro-climate and surface roughness, prevents avalanches formation and is able to stop movement of small avalanches due to higher friction in the transition- and the avalanche run-out zone (Schneebeli and Bebi, 2004; Bebi et al., 2009; Teich et al., 2012; Brožová et al., 2021). In order to take forest cover into account for hazard mapping, we used the algorithm developed by Bebi et al. (2021) and introduced by Bühler et al. (2022) for avalanche hazard mapping, to identify protective forest in the study area (Fig. 2). This algorithm is based on a database of 150 forest avalanches and yields a logistic regression model taking into account the parameters slope gradient, degree of forest cover and gap widths. Together with a vegetation height model (VHM) and a high resolution elevation model (DEM), a generated logistic regression model was used to calculate the avalanche disposition (Bebi et al., 2021). The so-derived protective forest was calculated for frequent (return periods < 100 years) and extreme scenarios (return period > 100 years). The protection

https://doi.org/10.5194/nhess-2022-112
Preprint. Discussion started: 6 April 2022


Natural Hazards and Earth System Sciences
Discussions

forest model (Fig. 2) is improved and extended by "shrub forest" (= additional bush forest) layer (Weber et al., 2020) and a ground roughness layer. This procedure results in a binary protection forest layer (green forest layer in Fig. 3) that divides the area of investigation into areas with and areas without protection forest (Bebi et al. (2021)). With a forest layer generated this way, it is assumed for the large-scale avalanche mapping process that an avalanche release in the forest is not possible (Bühler et al., 2018). The formation of avalanches is also prevented by infrastructure, such as areas with buildings or rail networks and roads. These constructed zones further subdivide avalanche release areas into smaller sub-areas. Therefore, they are also added to the binary layer as areas that prevent avalanche release.

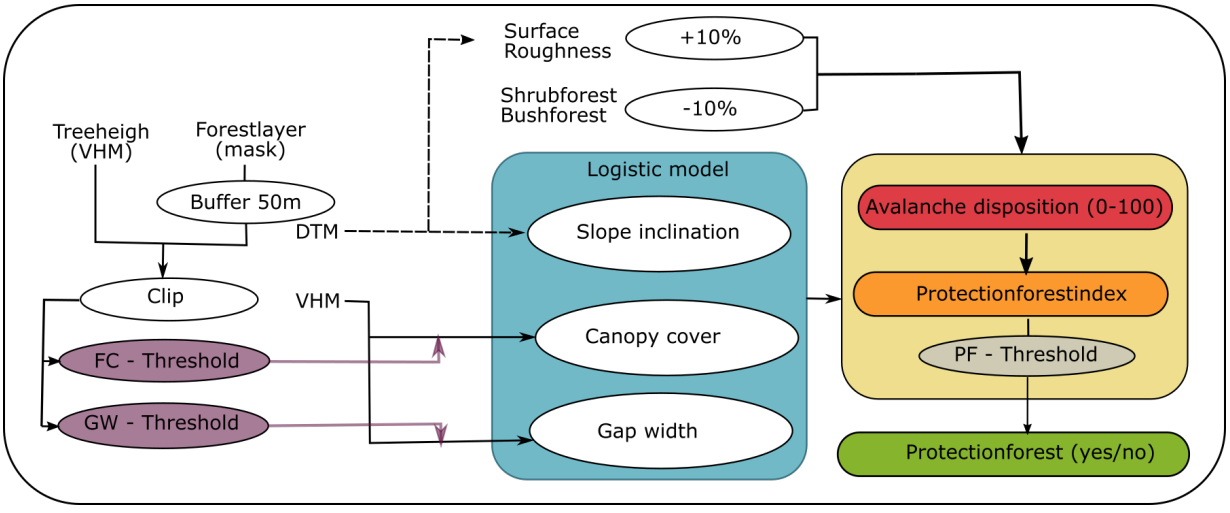


**Figure 2.** A schematic illustration of the python based forest model used for the calculation of the protection forest (PF) in the case study region. This model is based on a logistic model that represents avalanche formation in forest. GIS input data: a vegetation height model (VHM), a digital terrain model (DTM) and a shrub (bush) forest layer were used. FC = Forest cover, GW = Gap width, Fig. modified after Bebi et al. (2021).

For release volumes volume < 25'000 $m^3$, the binary forest layer as described above is considered for the simulations with assigned friction parameters mu (basal friction) and xi (turbulent friction). Values of mu = 0.020 and xi = 400 were assigned for the simulations in RAMMS::LSHIM, because protective forest has an strong influence on the friction during the run out of the avalanches in frequent scenarios with smaller avalanche volumes. For release areas with volumes > 25'000 $m^3$, the influence of the protective forest is neglected, since the energy generated during the flow process mostly destroys the protective forest and has often hardly any noticeable effect on the size of the affected area in the run out zone (Bartelt et al., 2017). In the extreme scenarios the tiny and small potential release zones are simulated with forest influence. In the frequent scenarios, on the other hand, the medium and large potential release areas are calculated also without forest.

https://doi.org/10.5194/nhess-2022-112
Preprint. Discussion started: 6 April 2022


Natural Hazards and Earth System Sciences
Discussions

### 2.1.2 Generation of automated avalanche release areas

In order to model the avalanche hazard, it is essential to correctly identify the potential avalanche release areas. In practice and for applications on single slopes, this is usually done individually by expert assessment considering geometrical properties of the avalanche prone slopes. This individual selection is no longer efficient for a large-scale application like in this study and was therefore done with an automated approach introduced by Maggioni and Gruber (2003) and further developed by Bühler et al. (2013); Veitinger et al. (2016); Bühler et al. (2018), applied to large scales by Bühler et al. (2022).

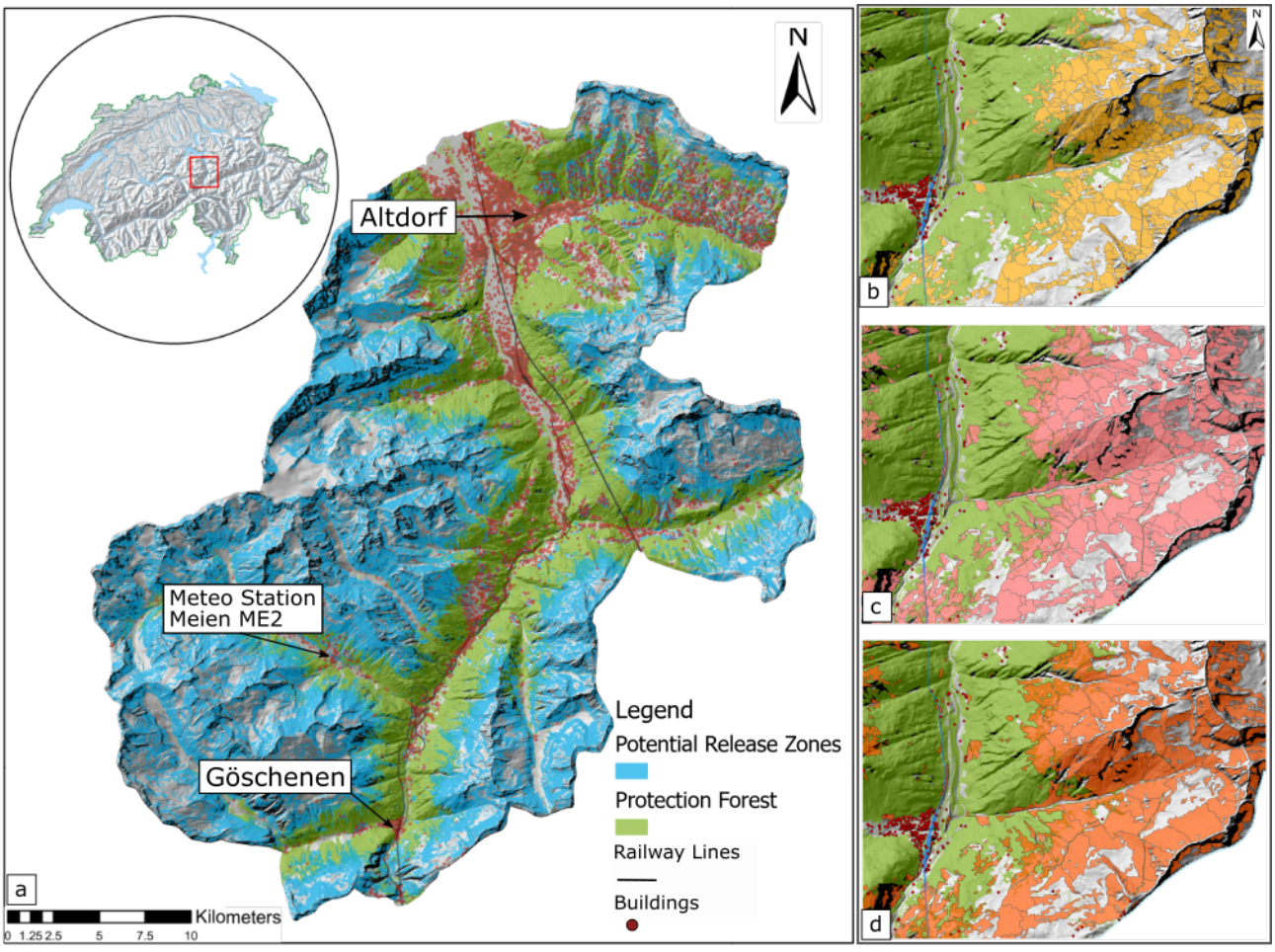


**Figure 3.** (a) Overview of the project area with the automatically generated protection forest layer in green and the area of potential avalanche release in blue, (b-d) automatically generated individual release areas (b) for a 30-year return period, (c) for a 100-year return period, (d) for a 300-year return period. Map base data source: Swiss Federal Office of Topography

This approach is based on a terrain analysis in a GIS and the "object based image classification OBIA" method (Blaschke, 2010) to delineate the individual release polygons, which serve as input for the large scale avalanche hazard indication mod-

https://doi.org/10.5194/nhess-2022-112
Preprint. Discussion started: 6 April 2022


elling (Bühler et al., 2013; Bühler et al., 2018). The algorithm analyses the slope geometry and identifies all possible potential avalanche release zones automatically for a given set of input data. With the automated processing, the single release areas are mapped and classified into four release area size classes: large (release volume > 60'000 $m^3$), medium (25'000 - 60'000 $m^3$), small (5'000 - 25'000 $m^3$)and tiny (< 5'000 $m^3$), depending on the initial scenario input definitions (see Fig. 3). Depending on these release volumes, different friction parameters are assigned to the associated avalanche for the subsequent simulation. These friction parameters mu (basal friction) and xi (turbulent friction) are assigned according to the RAMMS standard modelling procedure (Christen et al., 2011) which is known to be standard for hazard mapping in Switzerland.

#### 2.1.3 Definition of three avalanche scenarios

To cover a large range of potential avalanche events, we use 3 different avalanche scenarios (see Tab. 1). One frequent scenario [A] corresponding to a snowfall event with a 30-year return period, one intermediate [B] (100-year return period) and one extreme [C] scenario (300-year return period). The definition of the scenarios corresponds to the maximum 3-day snow depth increase and directly determines the mean fracture depths, thereby the release volume and thus the modelled avalanche run out lengths. The higher the return period, the larger the mean avalanche volume. The term return period (rp) describes the average number of years between two comparable events of the same intensity at the same location. By hazard frequency we denote the probability of occurrence calculated as reciprocal value of the return period (1/rp). This definition is common practice in avalanche hazard mapping (PLANAT, 2009; Salm et al., 1990).

The derivation of the 3-day snow depth increase was based on long-term snow measurement series at meteorological stations representative for the chosen area. As shown in Fig. 4, two extreme value statistic methods were applied: the generalized extreme value distribution with maximum likelihood estimations (GEV - MLE) and the Gumble distribution (Bocchiola et al., 2008) with maximum likelihood estimations (GUM-MLE). Table 1 shows that both methods produce similar values, but slightly higher values with GUM-MLE. This depends on the choice of the fitted correlation through the value distribution. Since the GUM distribution rather represents a "worst case" for the respective return period and Bocchiola et al. (2008) confirms the application of this method, these values were chosen for the fracture depth determination. To account for elevation of the release area, a correction factor has to be applied. Blanchet et al. (2009) estimated this factor to be about +/- 2 cm per 100 elevation meters, whereas Swiss practitioners usually use a gradient of 5 cm per 100 elevation meters (Margreth et al., 2008). In consideration of the large avalanche scenarios, we applied 5 cm per 100 elevation meters to each release polygon corresponding to further studies in the Swiss Alps (Bühler et al., 2022). For steeper terrain, we assumed that less snow accumulates than in flat terrain. This is applied automatically in the ArcGIS Python Script for fracture depth (d0) calculation by using the function $\psi = 0.219/sin(\alpha) - 0.202 \times cos(\alpha)$ with $\alpha$ being the slope angle (Bühler et al., 2018).

Snow depth increase data was taken from the SLF-station Meien ME2 (see Fig. 3). This station has a time series of 66 years and includes extreme snowfalls (e.g. winter 1950/51 and 1998/99) making the data basis more reliable for extreme events. It is located in the center of the project area at an altitude of 1320 m a.s.l., which is close to the average altitude of the release areas. Since the snow depth increase $\Delta$HS(3) (see Fig. 4) at the meteorological station Meien is taken in flat field, a standard slope inclination correction (Margreth, 2007) was conducted at all release polygons to consider an adapted fracture depth. In

https://doi.org/10.5194/nhess-2022-112
Preprint. Discussion started: 6 April 2022


Natural Hazards and Earth System Sciences
Discussions

**Table 1.** Δ 3-Days Snow height accumulation [cm] at the weather station Meien (1320 m a.s.l.) in canton of Uri.

| Scenario | Return Period | GEV-MLE [cm] | GUM-MLE [cm] |
|---|---|---|---|
| [A] | 30y | 112 | 114 |
| [B] | 100y | 130 | 136 |
| [C] | 300y | 147 | 156 |

order to correct for the influence of drifting snow, a snow drift factor was added depending on the size of the scenario (Salm et al., 1990). In practice, this factor strongly depends on local conditions at the release zones (Margreth, 2007). For the 30-year return period scenario we added 30 cm and for the 100y return period scenario 40 cm and the 300y return period scenario 50 cm of drifting snow correction. After defining the fracture depth and the area of the release zones as well as applying the corresponding correction factors, the volume for each release area could be determined and used for the hazard simulation with the RAMMS large scale hazard indication mapping model (Bühler et al., 2018, 2022).

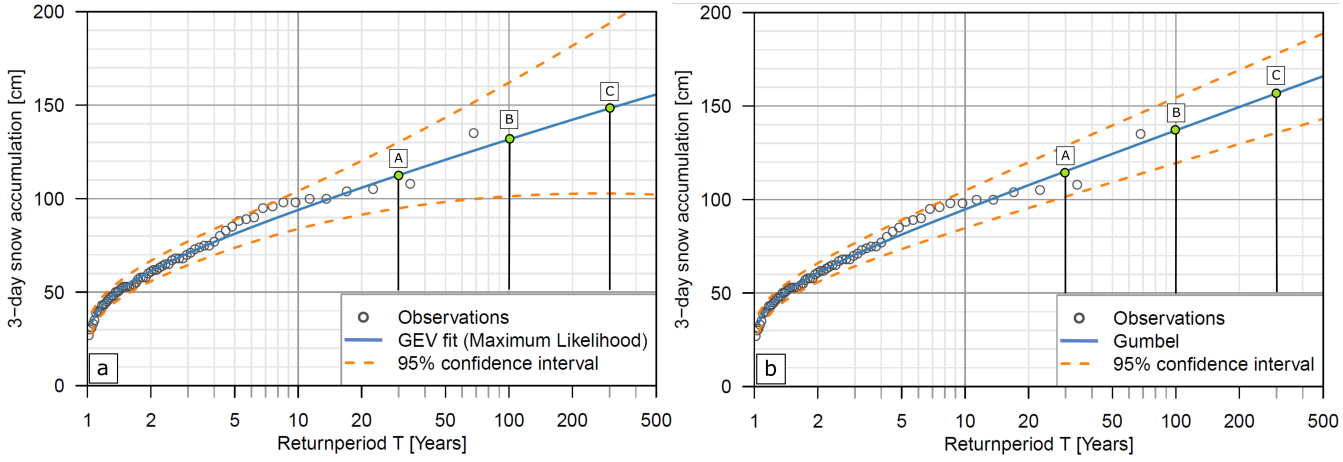


**Figure 4.** Extreme value statistics of the 3-day snow depth increase data (ΔHS3) of the meteo-station Meien (1320 m a.s.l.) for determining scenario return periods, Fig. 4(a): GEV-MLE Generalized extreme value distribution with maximum likelihood estimations for scenario [A] = 30, [B] = 100, [C] = 300; Fig. 4(b): GUM Gumble distribution with maximum likelihood estimations for scenario [A] = 30, [B] = 100, [C] = 300, see Tab. 1.

### 2.1.4 Large scale avalanche hazard indication mapping with RAMMS::AVALANCHE

RAMMS::AVALANCHE is numerical avalanche simulation model capable of simulating avalanches in complex topography (Christen et al., 2011). It is based on an efficient second-order numerical solution of the depth-averaged avalanche dynamics equations and the two parameter Voellmy model (Voellmy, 1955) and has been calibrated with numerous real observed avalanches such as for example at the SLF test site in Vallée la Sionne (community of Arbaz, Valais). We used

https://doi.org/10.5194/nhess-2022-112
Preprint. Discussion started: 6 April 2022


Natural Hazards and Earth System Sciences
Discussions

RAMMS:LSHIM, which is an adapted version of RAMMS::AVALANCHE, an extended set of algorithms for automatic release area identification (Bühler et al., 2018; Bühler et al., 2018; Bühler et al., 2022) and the standard friction parameter set, which is commonly used in practice (Christen et al., 2011; Gruber and Margreth, 2001). A three-dimensional digital terrain model with a spatial resolution of 10 m, the automated generated release areas and the fracture depth (Tab. 1) served as input to calculate the flow velocity, flow heights and the resulting impact pressure expressed in kPa of 40,000 single avalanches for all three scenarios (Bühler et al., 2022). Each avalanche was assigned to a release zone and individually saved as a separate file, which allowed us to allocate each avalanche with its pressure to a return period, which could later be used in a risk analysis. Figure 5 shows the resulting large-scale hazard indication map and in detail how the individual scenarios were simulated under the consideration of protection forest (Fig. 3).

https://doi.org/10.5194/nhess-2022-112
Preprint. Discussion started: 6 April 2022


Natural Hazards and Earth System Sciences
Discussions
Open Access
EGU

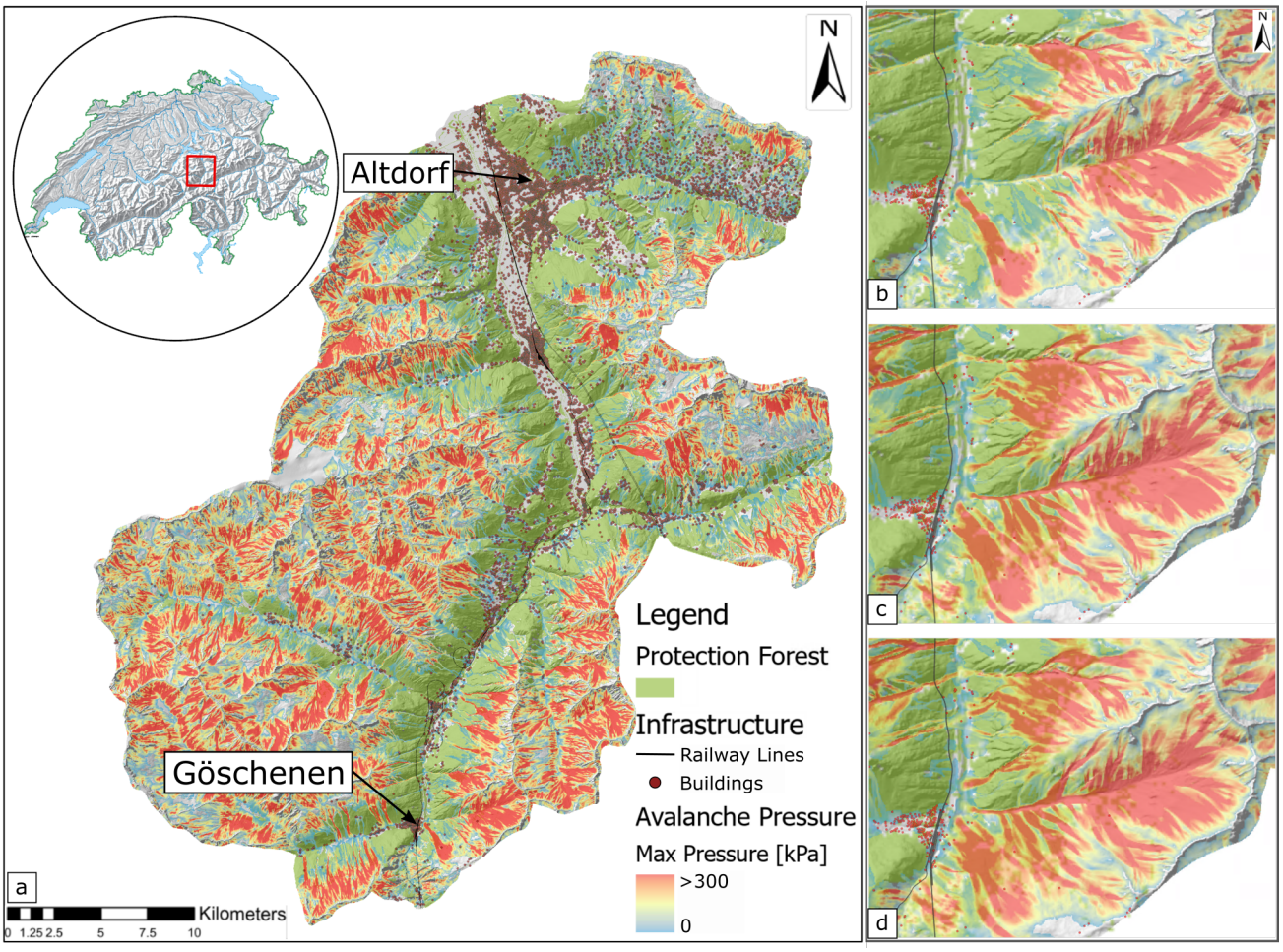


**Figure 5.** (a) Project area with results of the large scale avalanche simulation, pressure in [kPa], (b) detail of the simulation for the frequent scenario, corresponding to a 30y return period, (c) detail of the simulation for the large scenario, corresponding to a 100y return period, (d) detail of the simulation for the extreme scenario, corresponding to a 300y return period. Map base data source: Swiss Federal Office of Topography

## 2.2 Exposure

### 2.2.1 EconoMe

EconoMe is an online tool for the evaluation of the effectiveness and economic efficiency of mitigation measures against natural hazards (Bründl et al., 2016). It provides a sophisticated methodology for risk analysis and the evaluation of the cost-benefit-ratio of protective measures and is used by private companies, cantonal and federal authorities for decision support in

https://doi.org/10.5194/nhess-2022-112
Preprint. Discussion started: 6 April 2022


Natural Hazards and Earth System Sciences Discussions

the subsidization process. We used specific impact functions and building values following the EconoMe methodology as input values for the risk analysis in this study.

### 2.2.2 Generation of high-resolution exposure point data sets with monetary values

According to the guideline of the Swiss Federal Office for the Environment on risk overviews (FOEN, 2020), we generated a data set with assigned monetary values for 13,304 individual buildings. To create this monetary building layer, objects need to be classified by using different data sets (see Tab. 2). The classification is carried out by plotting the statistical data (STATPOP, FSO (2019)) of housing units (people per building) and employment data (STATENT: data set of industrial used objects, FSO (2019)) for industrially used buildings on a 2D building layer. The monetary values of buildings are assigned according to building types (Tab. 2) following the FOEN guideline. The number of persons in one building unit was assumed as 2.24 persons per unit (FOEN, 2021). Using this value and statistical STATPOP data (provided by Swiss federal office of statistics, FSO (2019)), which provide information on the number of persons in each building, we were able to determine the number of housing units (=HU) rounded to the next smaller number. Based on the number of housing units, a value of 650,000 CHF for one single residential buildings was assigned according to the EconoMe methodology. For buildings with HU > 1 a value of 550,000 CHF / HU was assigned.

Since there is no comprehensive data available for evaluating the value of companies and buildings, the STATENT (provided by the Swiss federal office of statistics, FSO (2019)) data set was used. This data provides building coordinates of each registered company in Switzerland. If one or more STATENT data points plot on the location of a building, this building was classified as a business building. The value corresponds to the volume of the building (FOEN, 2021), which was taken from the Swissbuildings3D dataset (Origin: Swiss federal office of topography, swisstopo) yielding a value of 280 CHF per $m^3$ volume.

For objects with the combined usage "business and living", on which both, the STATENT and STATPOP data points apply, the number of residential units was taken for the assignment of the monetary value, as it provides the higher values. Buildings, located within the Swiss building zone plan with no inhabitants and a volume of less than 100 $m^3$, were classified as uninhabited outbuildings with a value of 60,000 CHF per unit (garages and parking lots including vehicles).

Uninhabited outbuildings with a volume greater than 100 $m^3$ were classified as economically used buildings and their value was determined by the volume. The same applies to buildings that are located outside the building zone plan. If their volume is less than 100 $m^3$ they were classified as agricultural outbuildings with a value of 80 CHF/$m^3$. If their volume is greater than 100 $m^3$ they were classified as agricultural main buildings with a value of 180 CHF/$m^3$ (FOEN, 2020). This method provided an exposure data set with a monetary value for each individual building. Using the impact function assigned to each building type, it was possible to define the monetary damage for each building potentially affected by an avalanche.

https://doi.org/10.5194/nhess-2022-112
Preprint. Discussion started: 6 April 2022


Natural Hazards and Earth System Sciences
Discussions

**Table 2.** Overview of the basedata used for the creation the monetary building layer, definition of monetary values by building type, abbreviations: HU = Housing Unit, FSO = Swiss Federal Statistical Office, swisstopo = Swiss Federal Office of Topography swisstopo, ID = EconoMe Identification Number

| Building Type | EconoMe ID | CHF | Data Information | Data Origin |
|---|---|---|---|---|
| Single residential buildings | 1 | 650,000 / HU | Resident population per Building STATPOP | FSO |
| Multi residential buildings | 87 | 550,000 / HU | Resident population per Building STATPOP | FSO |
| Garage and parking | 4 | 60,000 / per piece | Construction zones of Switzerland | swisstopo |
| Industrial building | 6 | 280 / $m^3$ | Employed population per Building STATENT | FSO \swisstopo |
| Agricultural use | 2 | 180 / $m^3$ | Swiss BUILDINGS 3D | swisstopo |
| Barn | 3 | 80 / $m^3$ | Swiss BUILDINGS 3D | swisstopo |

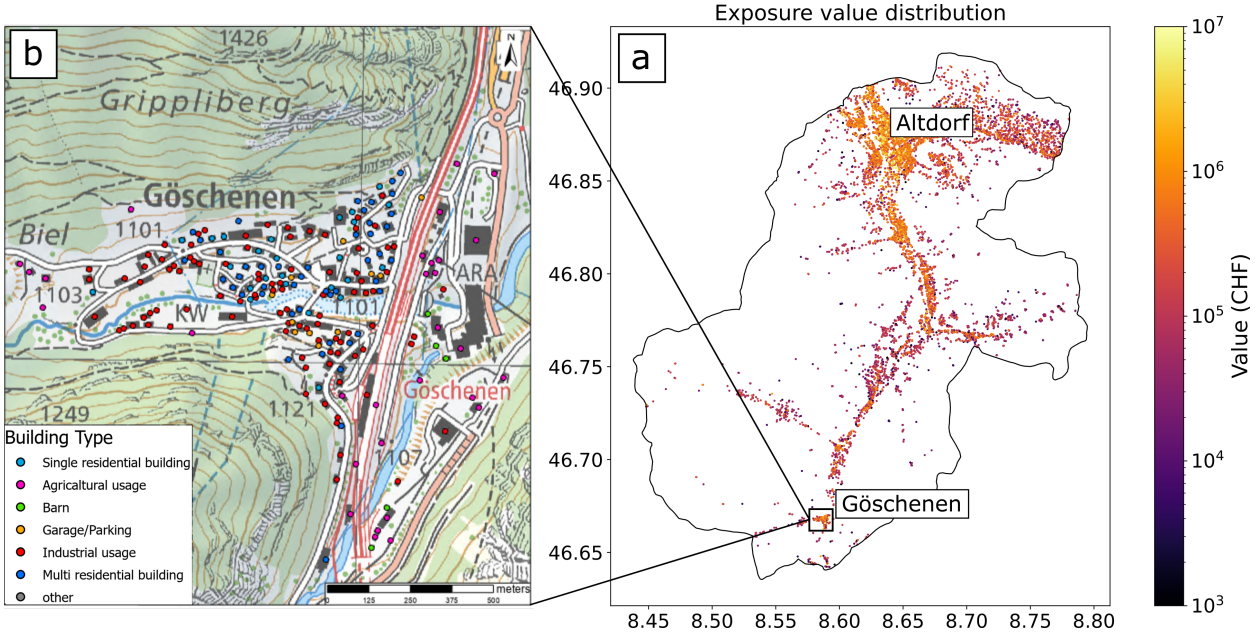


**Figure 6.** (a): Spatial distribution of exposed monetary values in the project area. (b): detail section, different building types matching actual buildings on the map (Map source: (a) CLIMADA python, (b) Swiss Federal Office of Topography, modified map)

## 2.3 Vulnerability

### 2.3.1 Avalanche impact functions

The extent to which an object is affected (damaged) by a hazard is referred to as the "hazard impact" or "impact". We determined the impact for avalanches using so called "impact functions", which is equivalent to "vulnerability function" or "damage function". We use impact functions as defined in the CLIMADA methodology (Aznar-Siguan and Bresch, 2019), which express

https://doi.org/10.5194/nhess-2022-112
Preprint. Discussion started: 6 April 2022


Natural Hazards and Earth System Sciences
Discussions

the damage an object suffers at a certain avalanche intensity (= pressure in kPa). These functions are based on values in EconoMe (FOEN, 2021). According to their type of construction, objects show a different damage susceptibility to avalanche pressure. We defined impact functions for each object type and combined them into a impact function set to describe the following avalanche impacts:

- the mean damage degree (MDD), expressing the mean percentage of damage (MDD) an object suffers under a certain avalanche impact pressure, expressed in kPa;
- the percentage of affected assets (PAA) in the hazard zone that suffer damage (100% in the case of avalanches), and
- the mean damage ratio at a certain pressure (MDR), in this study MDR = MDD.

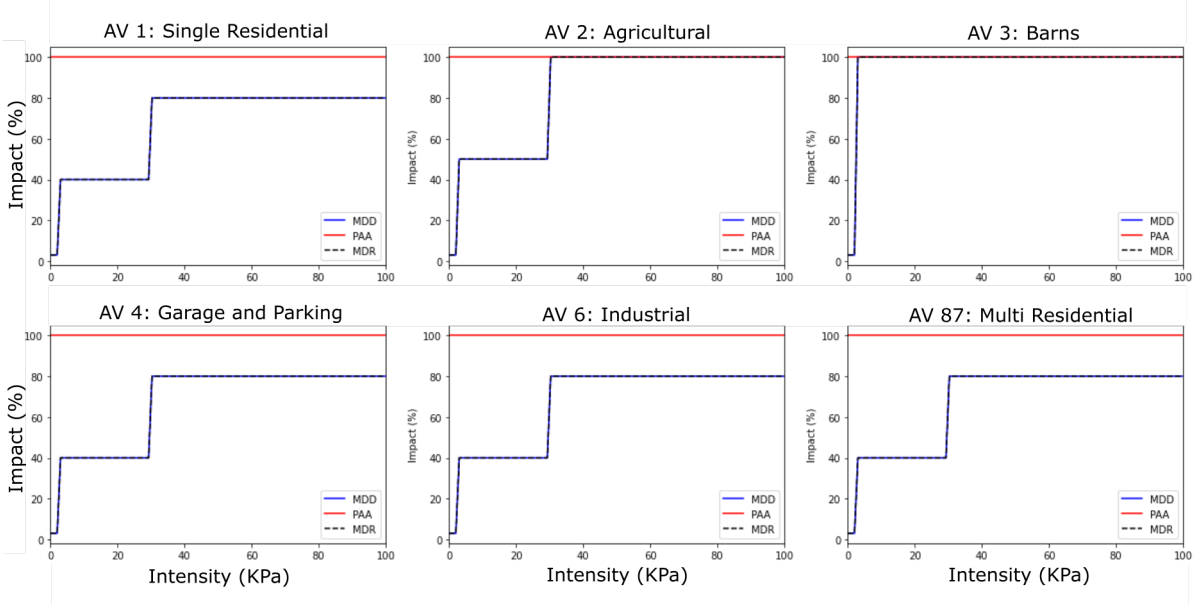


**Figure 7.** Impact functions showing the mean damage degree of different building types exposed to a certain intensity ( = mean avalanche pressure), PAA = 100%, MDR = MDD

Avalanche impact was categorized in the three classes low (0 - 3 kPa), medium (3 - 30 kPa) and extreme (>30 kPa) following the standards for hazard mapping in Switzerland (PLANAT, 2009, 2018).

## 2.4 Risk

### 2.4.1 CLIMADA

CLIMADA is an open-source and -access *Python* package for probabilistic risk assessment Aznar-Siguan and Bresch (2019). It allows for the computation of the impact of natural hazards, modelled as intensity maps, on exposures, modelled as value

https://doi.org/10.5194/nhess-2022-112
Preprint. Discussion started: 6 April 2022


Natural Hazards and Earth System Sciences Discussions

maps, considering the vulnerability of the exposures, modelled as impact functions. It is possible to compute the risk today and in the future, including climate changes that modifies the hazard and socio-economic development affecting the exposures and vulnerability. Finally, one can compute the reduction in risk and cost from adaptation options to perform a cost-benefit analysis Kropf et al. (2021). For all the model outputs, CLIMADA provides a module to perform uncertainty and sensitivity analysis Kropf et al. (2022) using global (quasi-)Monte-Carlo sampling.

In this project, we use CLIMADA to compute the risk of avalanches to more than 13'000 individual single buildings, from each of the 40,000 simulated avalanches using the hazard intensity maps described in Sect. 2.1, the exposures distribution described in Sec. 2.2 and the impact functions introduced in Sec. 2.3.1. As defined in the CLIMADA tool (Aznar-Siguan and Bresch, 2019), the impact is expressed by the following risk quantities:

- the expected annual impact (eai) for each exposure (affected building) expressed in monetary terms per year (CHF per year). It combines the hazard intensity with its expectation (= return period) and the damage degree from the impact functions;
- the average annual impact (aai) is the average of the expected annual impacts (eai) over all exposures, expressed in monetary terms per year (CHF per year);
- the average annual impact aggregated (aai_agg) is the sum of the average annual impacts (aai) for each scenario or all scenarios combined expressed in monetary terms per year (CHF per year). The aai_agg corresponds to the overall risk.

Furthermore, the uncertainties and sensitivity will be derived as described in the next Sects. 2.4.2 and 2.4.3. The uncertainty analysis describes the variability of the output of the model given a range for the input parameters, while a sensitivity analysis describes, how a certain uncertainty in the model can be assigned to a certain input parameter (Saltelli et al., 2019; Saltelli, 2002; Kropf et al., 2022). In this study, the model outputs of interest are the average annual impact aggregated over all exposure points for hazards with different return periods (c.f. Sect. 2.1.3). In general, it is not possible to consider the uncertainty in all the input parameters of a model such as CLIMADA (Otth et al., 2022). For this study, we focus the efforts on the total exposures value (building value), the mean damage degree thresholds of the impact functions (vulnerability), as well as the uncertainty of the intensity of the avalanches (impact pressure Sect.2.1) as discussed in details in the Uncertainty Sect. 2.4.2.

### 2.4.2 Uncertainty analyses

For the uncertainty analysis, a total of $N = 8000$ samples (see Fig. 8) of the uncertainty input parameters $ET, MDD, HI$ were generated using the Sobol sequence Kropf et al. (2022). The chosen uncertainty ranges are summarized in Tab. 3 and explained in details below. It is important to understand that the uncertainty ranges should not be interpreted as errors such as in the context of experimental measurement error, rather it is a description of a range of plausible model input values. It allows to gauge the robustness of the model and to obtain a spread of plausible risk outcomes Otth et al. (2022).

https://doi.org/10.5194/nhess-2022-112
Preprint. Discussion started: 6 April 2022


Natural Hazards and Earth System Sciences
Discussions

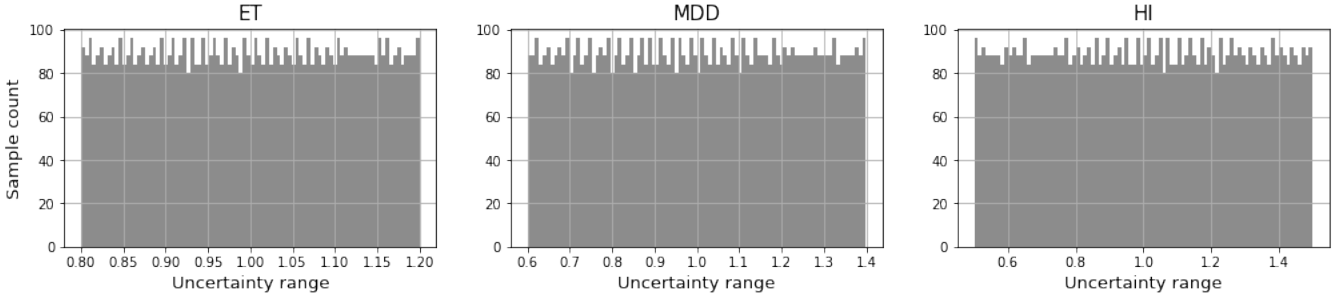


**Figure 8.** Generated samples for the chosen uncertainty variables ET = Exposure, MDD = Mean Damage Degree (impact function), HI = Hazard Intensity with a sample number of N = 8000.

Since the values of the exposure were determined with the generalized value assignment procedure introduced by FOEN (2020), it is clear that these can deviate from real life building values. Their method provides an estimation of a building value at a large scale, but cannot resolve the differences in value of similar building types. To account for the potentially large fluctuation in asset value, an uncertainty of $\pm 20\%$ of the total exposures value is assumed. In other words, for each run of the uncertainty sampling, all the assets value are multiplied with a value $ET$ uniformly sampled from $[0.8, 1.2]$. The obtained samples are illustrated in Fig. 8.

Industrial and residential buildings are the most costly building types. The steps of the impact functions for residential buildings and industrial differ by 40%. To cover a wide range of uncertainties, this value of the step jump in the function was taken as the possible uncertainty range. For agricultural buildings or outbuildings, this value can be even higher, as they often have a relatively simple construction. But due to their lower value they play a subordinate role. To define a "standard case" in our analysis, we consider the function steps of industrial or residential buildings as the variability range. Therefore, for the mean damage degree of the impact function a value range of $\pm 40\%$ was taken for the uncertainty analyses (c.f. Tab. 3). The obtained samples are illustrated in Fig. 8.

To define a range for the hazard intensity (HI) uncertainty analysis, we refer to data recorded in experiments at the Vallée de la Sionne test site. Sovilla et al. (2008a, b) have measured the impact pressure of dry, wet or mixed avalanches, which correspond to different flow regimes. However, in our simulations, we only simulated "dry avalanches", which have mostly higher velocities than 10 m/s. Pressure values of avalanches measured by Sovilla et al., show avalanche pressures in a range between 200 kPa and 700 kPa (Sovilla et al., 2008a). An extrapolation of the data set would yield maximum pressures of about 1000 kPa, which corresponds to the data obtained in our simulations shown in Fig. 5. The average pressure of the measurements would be around 600 kPa. Therefore, we assumed an uncertainty range of $\pm 50\%$ from the avalanche pressure (c.f. Tab. 3). The obtained samples are illustrated in Fig. 8.

https://doi.org/10.5194/nhess-2022-112
Preprint. Discussion started: 6 April 2022


**Table 3.** Uncertainties ranges of the chosen input parameters for the risk assessment

| Parameter | Uncertainty range |
|---|---|
| Exposure (ET) | 80% - 120% |
| Mean Damage Degree (MDD) | 60% - 140% |
| Hazard Intensity (HI) | 50% - 150% |

### 2.4.3 Sensitivity analysis

The sensitivity analysis determines which input parameter's uncertainty has the strongest influence on the model output uncertainties (Saltelli et al., 2019). In this study, we used the Sobol sensitivity indices as implemented in CLIMADA (Kropf et al., 2022), which can be computed from the same Sobol sequence as used for the uncertainty analysis (c.f. Fig.8). After the distribution of the impact metrics has been computed for all samples (see Sec. 3.2), the sensitivity index for the each metrics was computed. We considered the first order Sobol index S1 that describes the contribution of a single model input to the output variance.

## 3 Results

### 3.1 Risk maps

With the intersection of hazard maps, the objects at risk and the specific impact functions, we identified the spatial distribution of risk on large scale areas with the CLIMADA risk platform. More precisely, we are able to express risk measures such as the expected annual impact (eai) or the average annual impact (aai) for each individual object at a geographical location taking into account different synthetic hazard scenarios, and translate the damage into monetary terms per year (see Tab. 4). Figure 9, shows how different hazard scenarios affect single objects located in the hazardous area. Figure 9(a) represents the expected annual impact corresponding to a 30 year return period with an aai_agg (average annual impact aggregated) of CHF 5.02 million/year. Figure 9(b) displays the expected annual impact for single objects in an intermediate scenario with an corresponding return period of 100 years an average annual impact aggregated of CHF 4.6 million/year. Figure 9(c) shows the expected annual impact in the case of an extreme hazard scenario with a corresponding return period of 300 years for the single avalanches. The average annual impact (aai) calculated for the entire project area in this scenario is CHF 3.2 million/year. In a further step, we combined the three scenarios and adjusted them for combination with regard to the return period by $p_{30} = p_{30} - p_{100} = 1/30 - 1/100 = 0.0233$ and $p_{100} = p_{100} - p_{300} = 1/100 - 1/300 = 0.00667$ and $p_{300} = 1/300 = 0.0033$. This allows to express the expected annual impact (= eai) for single objects over all hazard scenarios combined. The representation of the expected annual impact in the entire project area, over all three hazard scenarios combined is depicted in Fig. 9(d) with an aggregated average annual impact (aai_agg) of CHF 9.73 million/year.

https://doi.org/10.5194/nhess-2022-112
Preprint. Discussion started: 6 April 2022


Natural Hazards and Earth System Sciences
Discussions

**Table 4.** Overview of the average damage and the rounded aggregated average annual impacts (aai_agg) for each of avalanche scenarios and all scenarios combined. The rounded aggregated average annual impact corresponds to the overall risk.

| Scenario | Average damage [million CHF] | Return period [years] | rounded aai_agg. [million CHF/year] |
|---|---|---|---|
| Small | 150.75 | 30 | 5.02 |
| Medium | 458.60 | 100 | 4.59 |
| Extreme | 947.12 | 300 | 3.16 |
| Combined | 1390.9 | all return periods | 9.73 |

As depicted in the risk maps of Fig. 9, it is striking that in all scenarios the most densely populated areas (see Fig. 6) in the main valleys do not represent the greatest risk accumulations in the maps. Hot spots are located on the slopes of the main Reuss valley near Wassen, Gurtnellen and in the side valleys near Meien. In these areas, alpine terrain with a high number of avalanche flow paths and a denser number of buildings overlap. There, the exposed buildings are mostly agricultural buildings. According to our method, the value of these buildings depend on their volume. Agricultural buildings can be large in volume, but are also very vulnerable to destruction by avalanches (see Fig. 7) due to their construction. This leads to high impacts at this locations as shown in Fig. 9. However, there are also a few multi-residential buildings in the endangered areas. If these buildings are at high risk, they appear on the map as dark dots. The largest accumulations of buildings at risk are found on the south-east to south-west facing slopes east of Altdorf. One explanation for this hot spot is the high number of agricultural buildings and a few residential buildings on very steep, avalanche prone, open slopes. The identification of such a hot-spots can play a crucial role in a decision making process as discussed in Sec. 5.

https://doi.org/10.5194/nhess-2022-112
Preprint. Discussion started: 6 April 2022


Natural Hazards and Earth System Sciences
Discussions

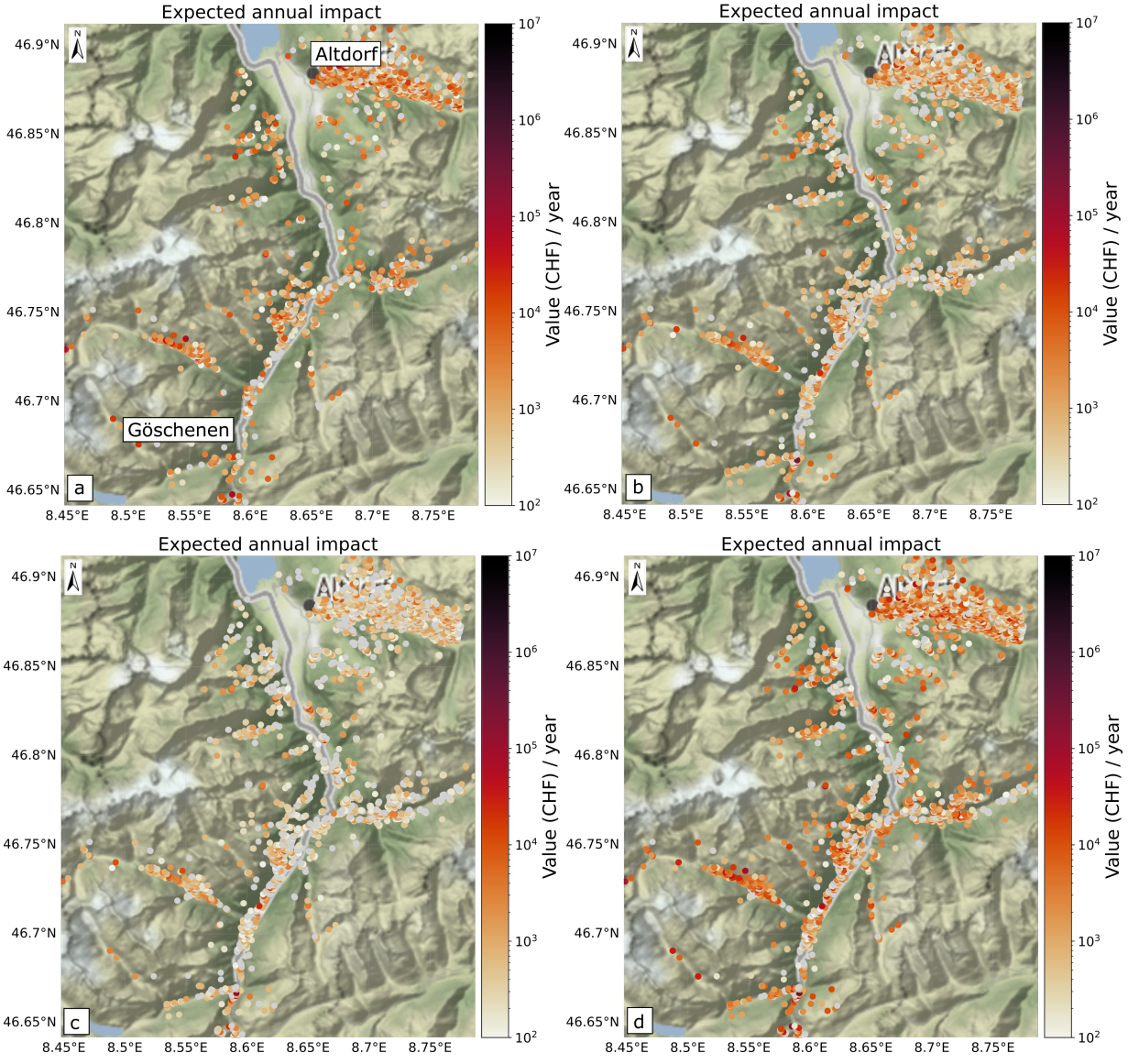


**Figure 9.** Risk maps: Overview of the spatial distribution of expected annual impact for individual objects at the three different avalanche scenarios (a) 30 return period, (b) 100 return period, (c) 300 return period (d) all hazard scenarios combined, Basemap origin (a-d): (a) CLIMADA, © OpenStreetMap contributors 2022. Distributed under the Open Data Commons Open Database License (ODbL) v1.0.

### 3.2 Impacts and uncertainty ranges

To account for the dispersion of risk under various uncertainties, the annual impact was calculated for randomly sampled cases falling within the defined uncertainty ranges. For the first event set with a 30y return period (Fig. 9(a)), the maximum density of samples histogram bars plot between CHF 3.4 million and CHF 5.6 million. This illustrates that the annual impact severity

https://doi.org/10.5194/nhess-2022-112
Preprint. Discussion started: 6 April 2022


for a hazard with a frequency of 1/30 is likely to lie in this range. The average annual impact values generally range from CHF 2.0 million to CHF 9.0 million. This means a wide dispersion of risk, yet it reflects the broad distribution of the exposed monetary values in the hazard area. Building values ranges from less than CHF 1,000 to maximum building values of CHF 78 million. The sample size was 8000 generated samples for each parameter and the impact was calculated for each of these samples. The histogram is not normally distributed, it shows a right skewed distribution with an average impact value of CHF 4.87 million with a standard deviation of CHF 1.34 million. Taking into account the uncertainties discussed above, it is very likely that, under the assumed model conditions, the annual risk across the entire area under investigation will be in the range CHF 3.4 million and CHF 5.6 million per year.

The situation is slightly different, however, for the scenario with a 100y return period despite higher avalanche pressures, the risk is lower and also with a lower variance. The explanation for this is the influence of the low hazard frequency, which significantly influences the risk. Taking into account the uncertainties, the possible annual impact in the project area is between CHF 2.9 million and CHF 5.4 million. The distribution extends almost over the same range as the 30y return period scenario, but with a sightly higher sample count of 3.5e-7. The average annual impact across all values inside the chosen uncertainty range for the 100y return period scenario is CHF 4.34 million with a standard deviation of CHF 1.11 million. The histogram for the 100y return period shows also a right skewed distribution and compared to the 30y return period distribution, it is almost equally distributed.

Looking at the distribution of the 300y return period scenario (Fig. 10(c)), we see that the average value of the annual impact is CHF 2.99 million with a standard deviation of 734.06 kCHF; the risk is significantly lower than in the 30y return period scenario and also lower than in the 100y return period scenario. The highest sample count is in a variability range of CHF 2.1 million and CHF 3.6 million. In principle, an avalanche scenario with a high return period cover a larger areas and/or, have a longer run out and a larger lateral spread and affect more objects and therefore cause higher damages. Although the damages in the 300y and 100y scenario are higher (see Tab. 4 and Fig. 11), the risk is lower because of the lower probability. This clearly shows two things: if we compare the annual impact of the 30y return period scenario with the 300y scenario, we see that the annual impacts of the 30y return period scenario are relatively high. The total damage caused by avalanches in the 30y return period scenario would be approx. CHF 150.8 million, for the 100y return period scenario, CHF 458.6 million and approximately CHF 947.1 million for the 300y return period scenario. For an overview of impacts and damages (= impact excluding return periods) please see Tab. 4.

In a further step, we combined the three avalanche scenarios and calculated the annual average impact aggregated for all samples (see Fig. 10). Here we see a significantly higher impact range of CHF 7.0 million to CHF 11.5 million with an average value of CHF 9.29 million and a standard deviation of CHF 2.41 million. This shows the great influence of the return period in the calculation of the risk. The risk of a 30y return period scenario can therefore be significantly greater than that of a 300y scenario. From the perspective of risk, one could conclude that it might make sense to protect the region against a 30y or a 100y return period scenario and thus reduce the effects of a much less likely 300y scenario considerably.

https://doi.org/10.5194/nhess-2022-112
Preprint. Discussion started: 6 April 2022


Natural Hazards and Earth System Sciences
Discussions

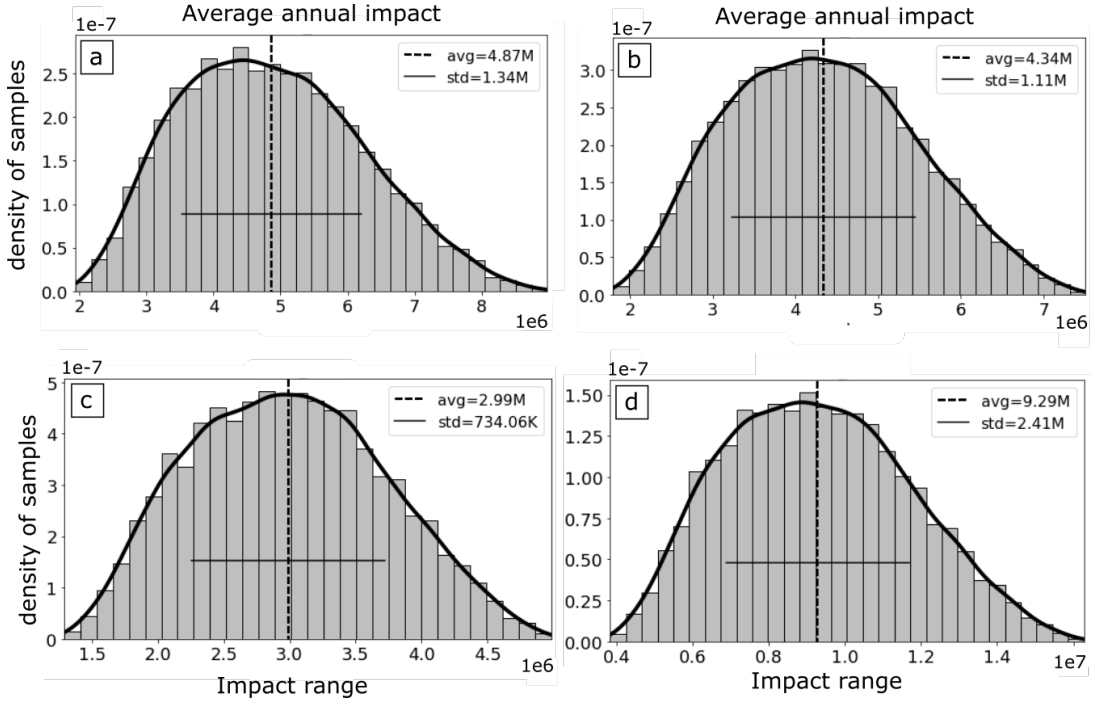


**Figure 10.** Calculated distribution of the average annual impacts from the scenarios (a) 30y (b) 100y (c) 300y (d) combined, for one eight-thousand randomly pulled samples within defined uncertainty ranges (Tab. 3). aai agg. = average annual impact aggregated impact value (summed over events and locations), avg = average, std = standard deviation

### 3.3 Damage frequency curve

In order to show the relation of the calculated impacts and their uncertainty distributions, on scenarios with other return periods, we produced a damage frequency curve for which we excluded the return period from the aggregated average annual impacts of the three scenarios (see Tab. 4) to obtain the average damage. For the three scenarios, we have plotted the damage against the return period (Fig. 11(a)). To incorporate the results of the uncertainty analysis in this curve, we calculated the 95th and 5th percentile of all damages of the three scenarios (again excluding the return period) of the uncertainty analysis. Thus, for the confidence interval calculation, eight-thousand values were available for each of the three return periods (30y, 100y, 300y). As shown in Tab. 4 and Fig. 11 the damage for a frequent (30y return period) scenario is about CHF 150.8 million with a variation from CHF 151 - 216 million (5th - 95th-percentile). In the 100y return period scenario the average damage is 458.6 million with a variation (5th - 95th-percentile) of about CHF 262 - 625 million. The higher the scenario, the more objects are affected and the larger are the uncertainties expressed in monetary terms. The 300y scenario shows an average damage of CHF 947.1 million with a large uncertainty range from CHF 548 million - 1.27 billion (5th - 95th-percentile). The dispersion of the uncertainty data for the return periods can be seen in Fig. 11(a) and (b). The median value (black line in the boxplots), calculated from all values of the uncertainty margin of the scenarios is compared with the average damage (see Tab.4 displayed

https://doi.org/10.5194/nhess-2022-112
Preprint. Discussion started: 6 April 2022


Natural Hazards and Earth System Sciences
Discussions

as black square in Fig. 11(b)). Figure 11(b) shows that the average damage values of the three single scenarios are close to the median values of the box plots calculated from all values including the uncertainty margin. It demonstrates that the original calculations for the single damage values are of good quality. Whether the interpolated damages from the scenarios that were not calculated in this study are in a linear relationship to the calculated damage is a rough assumption. Nevertheless, this curve can be used to infer approximate dimensions of the damage to be expected in other return periods, taking into account various uncertainties.

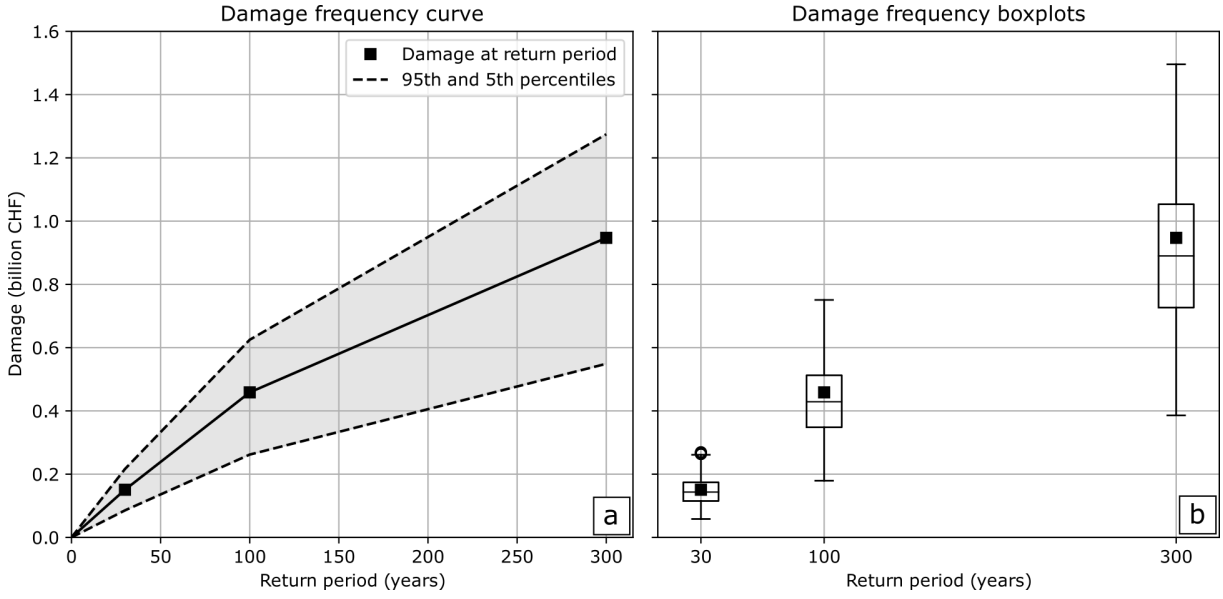


**Figure 11.** (a): Damage-Frequency curve showing the calculated damage at a certain return period with the 95th percentile of all damages calculated within the defined uncertainty ranges, (b): Boxplots of the 3 scenarios plotting all calculated damages of all uncertainty samples (black square = average damage (without return period) of the three scenarios. The boxes extend from [Q1] = first quartile to [Q3] = third quartile of the impacts at return period, the median is depicted as a line. The whiskers lines enhance from the box by 1.5 x the inter-quartile range (IQR). Points are data exceeding the end of the whiskers

### 3.4 Input parameter sensitivity analysis

As described in the methods section above (section 2.4.3), we calculated the first-order sensitivity index S1 to identify which parameter impacts the aggregated average annual impact most. Figure 12(a-c) shows that the mean damage degree MDD plays the most important role in this model for all scenarios. For the scenario with a return period of 30 years and the scenario with a return period of 100 years, the exposure ET and the hazard intensity HI seem to be almost equal. In the extreme scenario with a 300-year return period, significantly more objects are affected (see Fig. 9), and the exposure ET plays a slightly more important role here. The sensitivity index of the hazard intensity in the 30y and 100y return period scenario (Fig. 12(a) and 12b) is slightly higher than the S1 of the HI in the 300y return period scenario in Fig. 12(c). From this it can be concluded that

https://doi.org/10.5194/nhess-2022-112
Preprint. Discussion started: 6 April 2022


Natural Hazards and Earth System Sciences
Discussions

it is scenario dependent, whether the hazard intensity HI or the exposure ET have more influence. However, in all scenarios the mean damage degree MDD defined by the impact functions is the most influential parameter. For the combined hazard scenario (Fig. 12(d)) it is similar to the 300y return period scenario. Both the ET and the HI have the almost same high sensitivity index, but again the mean damage degree (MDD) is more influential.

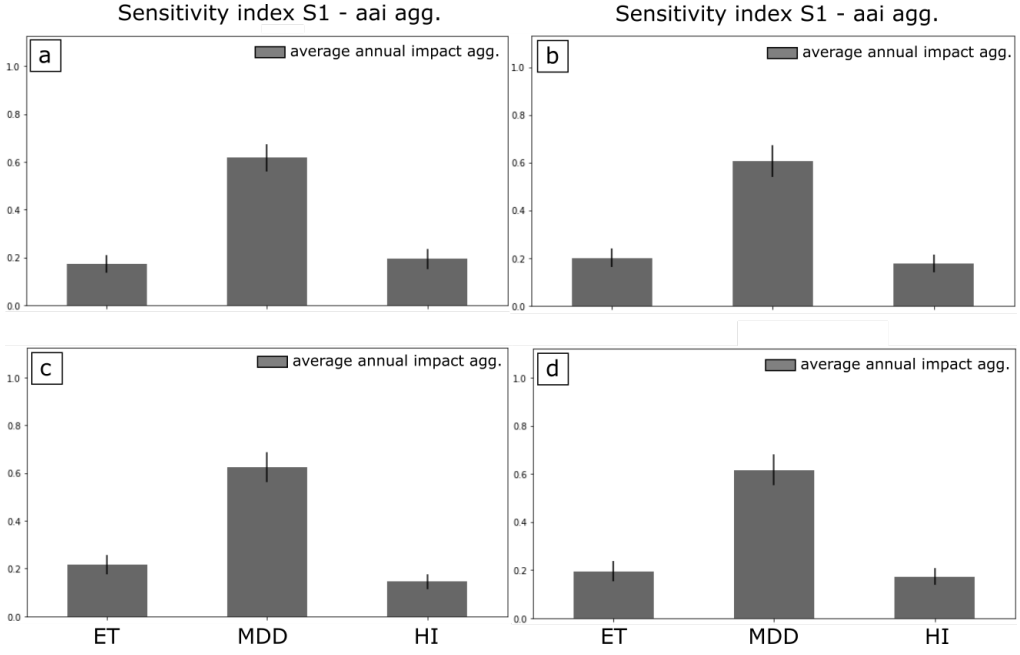


**Figure 12.** S1 - aai_agg = S1 first order sensitivity index and its effect on the average annual aggregated impact value (a) frequent hazard scenario, 30y return period (b) medium hazard scenario, 100y return period (c) extreme hazard scenario, 300y return period (d) over all combined

## 4 Discussion

### 4.1 Avalanche simulations

An avalanche hazard assessment in practice is a multi-step process based on a detailed analysis of the terrain characteristics, local records of snow precipitation data, documented previous events and expertise about the local hazard situation (Rudolf-Miklau et al., 2014). Avalanche release areas are manually identified by experts performing a detailed terrain assessment including an evaluation of protection forests, which is used as input for a numerical modelling of avalanche run out. In a large-scale avalanche hazard indication mapping, this detailed assessment process is largely omitted, which leads to some limitations (Bühler et al., 2022). Through the use of automated algorithms, release areas are only identified on the basis of terrain and scenario characteristics. This is an approximation, as actual avalanche release zones may vary in shape and size in nature. A validation of this algorithms has been carried out by Bühler and colleagues to evaluate the limitations of the object-based

https://doi.org/10.5194/nhess-2022-112
Preprint. Discussion started: 6 April 2022


image analysis (OBIA) approach (Bühler et al., 2018). These limitations are compensated by a fast and powerful applicability, which allows to map release areas at very large areas, where only the computational capacity and the computation time define the limits of its application. We considered the advantages of the large-scale applicability and the preciseness of the results corresponding to the goals of our study.

The automatic calculation of protection forest also entails its limitations. The definition of the protection forest was based on data sets compiled at a specific point in time in the past (2020) using remote sensing methods. With the effects of extreme windstorms or bark beetle infestations or consequences of climate change (e.g. dry periods), the forest structure can change rapidly (Brožová et al., 2020; Brožová et al., 2021). A detailed consideration of these effects and an expert evaluation of the protection forest (Bebi et al., 2021) is not appropriate for large-scale applications and not imperative for the creation of risk overviews. Our method is based on an evaluated approach for the definition of avalanche protection forest, has high quality standards and thus represents an essential basis for the delineation of avalanche release areas in our work.

In the present study, the avalanche fracture depth is extrapolated from the three-day snow depth increase of a single weather station located in the center of the project area. The three-day snow depth increase is determined using the extreme value statistics (GUM and GEV) (Bocchiola et al., 2008) and scenarios for three return periods are derived. This may result in uncertainties for both, the scenario definition and fracture depth, which have a direct effect on the avalanche volume and subsequently on the extent of the avalanches in the run out zones. The longer the time series, the more extreme events would have been recorded. However, a time series of 66 years used in our study is common practice (longer time series of data are not available), but it involves bigger uncertainties for estimation of fracture depths at high return periods. As can be seen in Fig. 4, the GEV method results in +/- 30cm for a 100y return period and +/- 50cm for a 300y return period, and the Gumbel method results in +/- 20cm for the 100 return period and +/- 25cm uncertainties for the 300y return period. Due to the 66-year record period, it can be assumed that the estimate of three-day snow depth increase for a 30-year scenario contains lower uncertainties (+/- 15 cm). This consideration of uncertainties does not yet take into account local wind effects that can arise because of the topography changes at ridges and mountain-backs that significantly influence snow deposition in the release areas. These effects can lead to a high variability of the snow pack in the release zones. However, these local conditions can't be taken into account in such large-scale applications. Only a wind load factor (30-50cm) depending on the scenario size was added. Without detailed wind/snow deposition studies, this uncertainty in the modelling process is hard to quantify and has to be accepted.

After all input variables have been determined in the avalanche simulation, the topography and the assigned friction parameters play the most important role in the run out flow of an avalanche. For single slope assessments, different parameters (mu and xi) would be assigned for each change in the flow cross-section (gully, channel or open slope) and thus detailed results could be approximated. In a large scale simulation, a generalized approach is used that regulates the friction parameters via the avalanche volume and takes the topography in the runout into account, but without manually assessed details (for details please see (Bühler et al., 2022)). This leads to a less differentiated hazard picture compared to a single slope approach in the

https://doi.org/10.5194/nhess-2022-112
Preprint. Discussion started: 6 April 2022


avalanche run-out zone. Another effect that includes uncertainties is that all geometrically possible release areas are simulated with our model. In reality, a more differentiated picture of avalanches would result for each catchment zone in which some release areas produce an avalanche and others do not. Over an entire catchment area, this leads to an overestimation of avalanche risk because of the avalanche release probability. It is not uniform for each slope aspect or catchment area. As far as we know, however, there are no studies on the release probability of avalanches, that can be applied to large scales to represent an actual natural avalanche release scenario in a model. The advantage of our approach, however, is that all avalanche areas that could geometrically produce an avalanche are actually covered in the simulation and taken into account for risk assessment. Here the need for further research is identified in order to design probabilistic avalanche sets to cover real life avalanche release scenarios. In our risk analysis, each individual avalanche is treated as an individual, independent event and the resulting damage is averaged out over all events impacting an object.

### 4.2 Building impacts and avalanche risk mapping

In this paper we identify the monetary avalanche risk on a large scale for buildings. We intersect impact functions with defined vulnerabilities of buildings with monetary values and continuous hazard indication maps of avalanche pressure. In order to do this on a large scale, some generalisations have to be done which leads to certain limitations in the level of detail.

The impact functions define the damage rate in steps and pressure classes. Actual damage does not always depend on these classes. If an avalanche hits an object, it is important at what angle the building is oriented in relation to the flow direction of the avalanche, the specific flow regime as well as how high the avalanche flows (Kyburz et al., 2018) or whether the building has structural weakness points (e.g. windows or doors) exposed to the avalanche flow. Even though the development of these steps was derived from expert assessments and damage surveys of avalanche incidents, it is unlikely that real damage always follows these steps or is linear to the avalanche pressure - this depends strongly on the individual situation. Even minor damage to the foundations of a house can lead to total damage and reconstruction. In our method, all these details cannot be taken into account. To ensure the performance of our approach, we generalize. We consider buildings as point objects with a generalised vulnerability. This allows an efficient large-scale approach but introduces inaccuracies in detail. However, we try to address the framework of these uncertainties by means of overall uncertainty analysis.

Further, the method of the avalanche impact calculation does not take into account the temporal effects of the hazard. In reality, the first avalanche that destroys an object completely, "prevents" its destruction by further events. After many minor avalanches at the exact same catchment area, the probability of a major event at the same location decreases. To cover these effects in a risk tool, a detailed probabilistic study would be needed for each individual catchment area. Local meteorological weather events and time-dependent interactions of individual avalanches would have to be investigated in detail. This would increase the level of detail but significantly weaken the independence of the place of application as well as the large-scale applicability for the identification of avalanche risks.

https://doi.org/10.5194/nhess-2022-112
Preprint. Discussion started: 6 April 2022


In this work, we have linked a risk tool with a new method for hazard assessment. We have calculated and presented avalanche risks of over 40,000 single avalanches in different hazard scenarios for more than 13,300 buildings over an area of 469.3 $km^2$. Due to the complexity and small scale of the hazard process, avalanche risk assessment is often addressed at the local level. Studies previously carried out in this field, such as that of Fuchs et al. (2004) and Fuchs et al. (2006) or more recent studies such as Zgheib et al. (2020) have put their focus on the scale of particular villages. Large scale approaches as the one of Kazakova et al. (2017) assess risk for 60 buildings, others out their focus on risks and forest (Renner and Steger, 2021) . Fuchs et al. (2015) uses detailed avalanche hazard maps at regional scale and flood hazards on countrywide scale. If one compares the method we use, avalanche danger can be modeled for unlimited sized territories with little time expenditure, without using hazard maps previously provided by local authorities. Exposure values can also be generated in CLIMADA via night light assessments if no detailed information on buildings is available (Aznar-Siguan and Bresch, 2019). The RAMMS::LSHIM method and the good adaptability of the risk tool is a significant advantage when applying this method in areas where there is no or limited hazard or asset information available.

## 5 Conclusions and outlook

Our novel approach for simulating avalanches and assessing the spatially distributed risk through monetary valuation is valid at large scales with a high degree of detail (single-object-resolution). Owing to the avalanche simulations from the RAMMS:LSHIM method, no external avalanche hazard information is needed. Additionally, this concept can easily be adapted for different hazards or exposure scenarios. It provides an overview of objects within an area which are threatened by natural hazards, and helps practitioners to identify risk hot spots and previously unknown threats. Thus, the process presented in this paper serves to pinpoint locations of high risk where focused assessments might be necessary for hazard adaptation and mitigation.

This approach can be applied globally over large areas and could become particularly useful when considering anticipated future changes of risk. As such, studying hazard changes brought on by climate change or socio-economic shifts, where hazard assessments are missing, is a possible application for this analysis. Lastly, it can be applied in the context of a probabilistic options appraisal concerning risk reduction measures and adaptation planning. In a subsequent study, we will apply our approach to investigate the impact of climate change on future avalanche risk.

*Code and data availability.*

The potential release areas necessary for the reproduction of the hazard simulation and RAMMS simulations described in this paper are publicly available on ENVIDAT www.envidat.ch, the WSL data portal with the final submission.
CLIMADA is openly available from GitHub https://github.com/CLIMADA-project/climada_python, B(Aznar-Siguan and Bresch, 2019)) under the GNU GPL license (GNU Operating System, 2007). The documentation is hosted on Read the Docs https://climada-python.readthedocs.io/en/stable/, (Aznar-Siguan and Bresch, 2019)) and includes a link to the interactive tutorial for

https://doi.org/10.5194/nhess-2022-112
Preprint. Discussion started: 6 April 2022


CLIMADA. CLIMADA, which is permanently available at the ETH Data Archive https://zenodo.org/record/5555825 ((Kropf et al., 2021)). The script reproducing the main results of this paper will be available at https://github.com/CLIMADA-project/climada_papers after the final submission.

*Author contributions.* G.O. and M.B. and C.M.K. designed the study, G.O. and C.M.K. performed the calculations. G.O., D.N.B., T.R. and C.M.K. programmed parts and/or made adaptations of the used risk assessment platform. Y.B. programmed and provided the necessary hazard mapping algorithm G.O. performed the hazard mapping and risk assessment. All authors contributed to the writing process and the validation of the paper, reviewed the results and proposed improvements.

*Competing interests.* The authors declare that they have no conflict of interest.

*Acknowledgements.* This work is funded by the WSL research program Climate Change Impacts on Alpine Mass Movements – CCAMM ccamm.slf.ch and the Swiss Railway Company SBB www.sbb.ch/en; we thank both for the financial support. We like to thank the WSL Institute for Snow and Avalanche Research SLF and ETH Zürich for providing their infrastructure and the great work environment, Marc Christen for adjustments to the RAMMS::Avalanche software, Peter Bebi and Gregor Schmucki for providing the forest layer methodology, and Stefan Margreth, Perry Bartelt, Lukas Stoffel, Linda Zaugg-Ettlin, Jan Kleinn, Michael Kyburz, Michael Lehning, Pius Krütli for their opinions and feedback. Christoph Marty for meteorological data delivery. We further thank Andreas Stoffel for ArcGIS support and Natalie Brozová, Dylan S. Reynolds and Michael T. Lombardo for code troubleshooting and scientific exchange.

https://doi.org/10.5194/nhess-2022-112
Preprint. Discussion started: 6 April 2022


## References

ASTRA: Naturgefahren auf den Nationalstrassen: Risikokonzept, Tech. Rep. 2, Bundesamt für Strassen ASTRA Abteilung Strassennetze N Standards und Sicherheit der Infrastruktur SSI, 2012.

Aznar-Siguan, G. and Bresch, D. N.: CLIMADA v1: a global weather and climate risk assessment platform, Geoscientific Model Development, 12, 3085–3097, https://doi.org/10.5194/gmd-12-3085-2019, 2019.

Ballesteros-Cánovas, J. A., Trappmann, D., Madrigal-González, J., Eckert, N., and Stoffel, M.: Climate warming enhances snow avalanche risk in the Western Himalayas, Proceedings of the National Academy of Sciences, 115, 3410–3415, https://doi.org/https://doi.org/10.1073/pnas.1716913115, 2018.

Bartelt, P., Christen, M., Bühler, Y., Deubelbeiss, Y., Salz, M., Schneider, M., and Schumacher, L.: RAMMS::AVALANCHE User Manual, WSL Institute for Snow and Avalanche Research SLF, v1.7.0 edn., 2017.

Bebi, P., Bast, A., Helzel, K., Schmucki, G., Brozova, N., and Bühler, Y.: Avalanche Protection Forest: From Process Knowledge to Interactive Maps, in: Online First, IntechOpen, https://doi.org/DOI: 10.5772/intechopen.99514, 2021.

Bebi, P., Kulakowski, D., and Rixen, C.: Snow avalanche disturbances in forest ecosystems-State of research and implications for management, FOREST ECOLOGY AND MANAGEMENT, 257, 1883–1892, https://doi.org/10.1016/j.foreco.2009.01.050, International-Union-of-Forestry-Research-Organization Conference on Natural Hazards and Natural Disturbances in Mountain Forests, Trento, ITALY, SEP, 2007, 2009.

Blanchet, J., Marty, C., and Lehning, M.: Extreme value statistics of snowfall in the Swiss Alpine region, Water Resources Research, 45, https://doi.org/https://doi.org/10.1029/2009WR007916, 2009.

Blaschke, T.: Object based image analysis for remote sensing, ISPRS J. Photogramm 65, 2–16, 2010.

Bocchiola, D., Bianchi Janetti, E., Gorni, E., Marty, C., and Sovilla, B.: Regional evaluation of three day snow depth for avalanche hazard mapping in Switzerland, Natural Hazards and Earth System Sciences, 8, 685–705, https://doi.org/10.5194/nhess-8-685-2008, 2008.

Borter, P.: Risikoanalysen bei gravitativen Naturgefahren– 107/1–Methode, Umwelt-Materialien 107/1, Tech. rep., Bundesamt für Umwelt, Wald und Landschaft, BUWAL, Bern, 1999.

Borter, P. and Bart, R.: Risikoanalysen bei gravitativen Naturgefahren–107/2–Fallbeispiele und Daten, UmweltMaterialien 107/2, Tech. rep., Bundesamt f¨ur Umwelt, Wald und Landschaft, BUWAL, Bern, 1999.

Brožová, N., Baggio, T., D'Agostino, V., Bühler, Y., and Bebi, P.: Multiscale analysis of surface roughness for the improvement of natural hazard modelling, Natural Hazards and Earth System Sciences, 21, 3539–3562, https://doi.org/10.5194/nhess-21-3539-2021, 2021.

Brožová, N., Fischer, J.-T., Bühler, Y., Bartelt, P., and Bebi, P.: Determining forest parameters for avalanche simulation using remote sensing data, Cold Regions Science and Technology, 172, 102 976, https://doi.org/https://doi.org/10.1016/j.coldregions.2019.102976, 2020.

Bründl, M., Krummenacher, B., and Merz, H. M.: Decision making tools for natural hazard risk management-Examples from Switzerland, in: Proceedings of the Joint ESREL and SRA-Europe Conference , Vol. 4, vol. 4, pp. 2773–2779, https://www.scopus.com/inward/record.uri?eid=2-s2.0-77949495122&partnerID=40&md5=f7316416fee08698ef89c39bd518fb0d, 2009.

Bründl, M., Baumann, R., Burkard, A., Dolf, F., Gauderon, A. andGertsch, E., Gutwein, P., Krummenacher, B., Loup, B., Schertenleib, A., Oggier, N., and Zaugg-Ettlin, L.: Evaluating the Effectiveness and the Efficiency of Mitigation Measures against Natural Hazards, Hazards. Koboltschnig, G. (ed), pp. 27-33, International Research Society INTERPRAEVENT, Lucerne, Switzerland., 2016.

Bründl, M., Hafner, E., Bebi, P., Bühler, Y., Margreth, S., Marty, C., Schaer, M., Stoffel, L., Techel, F., Winkler, K.and Zweifel, B., and Schweizer, J.: Ereignisanalyse Lawinensituation im Januar 2018, Tech. rep., Institut für Schnee und Lawinenforschung SLF, 2019.

https://doi.org/10.5194/nhess-2022-112
Preprint. Discussion started: 6 April 2022




Bühler, Y., von Rickenbach, D., Stoffel, A., Margreth, S., Stoffel, L., and Christen, M.: Automated snow avalanche release area delineation – validation of existing algorithms and proposition of a new object-based approach for large-scale hazard indication mapping, Natural Hazards and Earth System Sciences, 18, 3235–3251, https://doi.org/10.5194/nhess-18-3235-2018, 2018.

Bühler, Y., Bebi, P., Christen, M., Margreth, S., Stoffel, L., Stoffel, A., Marty, C., Schmucki, G., Caviezel, A., Kühne, R., Wohlwend, S., and Bartelt, P.: Automated avalanche hazard indication mapping on state wide scale, Natural Hazards and Earth System Sciences Discussions, 2022, 1–22, https://doi.org/10.5194/nhess-2022-11, 2022.

Bühler, Y., Kumar, S., Veitinger, J., Christen, M., and Stoffel, A.: Automated identification of potential snow avalanche release areas based on digital elevation models, Nat. Hazards Earth Syst. Sci., 13, 1321–1335, 2013.

Bühler, Y., von Rickenbach, D., Christen, M., Margreth, S., Stoffel, L., Stoffel, A., and Kühne, R.: Linking modelled potential release areas with avalanche dynamic simulations: An automated approach for efficient avalanche hazard indication mapping, Linking modelled potential release areas with avalanche dynamic simulations: An automated approach for efficient avalanche hazard indication mapping, 2018.

CH2018: CH2018 – Climate Scenarios for Switzerland, Tech. rep., National Centre for Climate Services, Zurich, 271 pp., https://www.nccs.admin.ch/dam/nccs/de/dokumente/website/klima/CH2018_Technical_Report.pdf.download.pdf/CH2018_Technical_Report.pdf, 2018.

Christen, M., Kowalski, J., and Bartelt, P.: Erratum to "RAMMS: Numerical simulation of dense snow avalanches in three-dimensional terrain" [Cold Regions Science and Technology, Volume 63/1–2 (2010) pp. 1–14], Cold Regions Science and Technology, 65, 273, https://doi.org/https://doi.org/10.1016/j.coldregions.2010.09.006, 2011.

FOEN: Minimale Standards Kantonale Risikoübersichten für gravitative Naturgefahren, Tech. rep., Federal Office for Environment Department Hazard Prevention, https://www.bafu.admin.ch/dam/bafu/de/dokumente/naturgefahren/fachinfo-daten/minimale_standards_kantonaler_risikouebersichten.pdf.download.pdf/minimale_standards_kantonale_risiko%C3%BCbersichten.pdf, 2020.

FOEN: EconoMe, Wirksamkeit und Wirtschaftlichkeit von Schutzmassnahmen gegen Naturgefahren., Federal Office for the Environment, Bern. www.economе.admin.ch (Last access: 28th Mach 2021)., 2021.

FSO: Federal Statistical Office: STATPOP and STATENT Data STATPOP: Individuals, households and economically active persons within the permanent and non permanent resident population (at their main residence and, if it applies, at their secondary residence), linked to georeferenced buildings and dwellings https://www.bfs.admin.ch/bfs/en/home/statistics/population/surveys/statpop.html STATENT: The statistics on the structure of enterprises (STATENT) provide central information on the structure of the Swiss economy, linked to georeferenced buildings and dwellings, Data delivery, https://www.bfs.admin.ch/bfs/en/home/services/geostat/swiss-federal-statistics-geodata/business-employment/structural-business-statistics-statent-from-2011-onwards.html, 2019.

Fuchs, S., Bründl, M., and Stötter, J.: Development of avalanche risk between 1950 and 2000 in theMunicipality of Davos, Switzerland, Natural Hazards and Earth System Sciences, 2004.

Fuchs, S., Keiler, M.and Zischg, A., and Bründl, M.: RISK21 - coping with risks due to natural hazards in the 21st century. Proceedings of the RISK21 workshop, chap. Temporal variability of damage potential in settlements – A contribution towards the long-term development of avalanche risk, p. 12, CRC Press In W. J. Ammann, S. Dannenmann, & L. Vulliet (Eds.), https://doi.org/https://doi.org/10.1201/9780203963562, 2006.

Fuchs, S., Keiler, M., and Zischg, A.: A spatiotemporal multi-hazard exposure assessment based on property data, Natural Hazards and Earth System Sciences, 15, 2127–2142, https://doi.org/10.5194/nhess-15-2127-2015, 2015.

https://doi.org/10.5194/nhess-2022-112
Preprint. Discussion started: 6 April 2022


Natural Hazards and Earth System Sciences Discussions

Fuchs, S., Heiser, M., Schlögl, M., Zischg, A., Papathoma-Köhle, M., and Keiler, M.: Short communication: A model to predict flood loss in mountain areas, Environmental Modelling & Software, 117, 176 – 180, https://doi.org/https://doi.org/10.1016/j.envsoft.2019.03.026, 2019.

Gruber, U. and Margreth, S.: Winter 1999: a valuable test of the avalanche-hazard mapping procedure in Switzerland, Ann. Glaciol, 32, 328–332, 2001.

Harvey, S., Schmudlach, G., Bühler, Y., Dürr, L., Stoffel, A., and Christen, C.: Avalanche terrain maps for backcountry skiing in switzerland, International Snow Science Workshop ISSW, Innsbruck, Austria, 2018.

Heinimann, H., Hollenstein, K. Kienholz, H., and Krummenacher, B. Mani, P.: Methoden zur Analyse und Bewertung von Naturgefahren - Eine risikoorientierte Betrachtungsweise, Tech. rep., BUWAL, 1998.

IPCC: Managing the Risks of Extreme Events and Disasters to Advance Climate Change Adaptation, A Special Report of Working Groups I and II of the Intergovernmental Panel on Climate Change by: Field, C. B., Barros V. Stocker T. F. Qin D. Dokken D. J. Ebi K. L. Mastrandrea M. D. Mach K. J. Plattner G.-K. Allen S. K. Tignor M. and Midgley, P.M.(eds.), Cambridge University Press, Cambridge, UK, and New York, NY, USA, 582 pp., https://www.ipcc.ch/report/managing-the-risks-of-extreme-events-and-disasters-to-advance-climate-change-adaptation/, 2012.

IPCC: Climate Change 2014: Impacts, Adaptation and Vulnerability. Part A: Global and Sectoral Aspects. Contribution of Working Group II to the Fifth Assessment Report of the Intergovernmental Panel on Climate Change, edited by: Field, C. B., Barros, V. R., Dokken, D. J., Mach, K. J., Mastrandrea, M. D., Bilir, T. E., Chatterjee, M., Ebi, K. L., Estrada, Y. O., Genova, R. C., Girma, B., Kissel, E. S., Levy, A. N., MacCracken, S., Mastrandrea, P. R., and White, L. L., Tech. rep., Cambridge University Press, United Kingdom and New York, NY, USA, 2014., https://www.ipcc.ch/report/ar5/wg2/, 2014.

Kappes, M. S., Keiler, M., von Elverfeldt, K., and Glade, T.: Challenges of analyzing multi-hazard risk: a review, Natural Hazards, 64, 1925–1958, https://doi.org/10.1007/s11069-012-0294-2, 2012.

Kazakova, E., Lobkina, V., Gensiorovskiy, Y., and Zhiruev, S.: Large-scale assessment of avalanche and debris flow hazards in the Sakhalin region, Russian Federation, Natural Hazards, 88, 237–251, https://doi.org/10.1007/s11069-016-2431-9, 2017.

Komendantova, N., Scolobig, A., Garcia-Aristizabal, A., Monfort, D., and Fleming, K.: Multi-risk approach and urban resilience, International Journal of Disaster Resilience in the Built Environment, 7, 114–132, https://doi.org/10.1108/IJDRBE-03-2015-0013, 2016.

Kropf, C. M., Schmid, E., Aznar-Siguan, G., Eberenz, S., Vogt, T., Steinmann, C. B., Röösli, T., Lüthi, S., Sauer, I., Mühlhofer, E., Hartman, J., Guillod, B. P., Stalhandske, Z., Ciullo, A., Kam, P. M. M., Fairless, C., Wüthrich, J., Meiler, S., Bungener, R., Bozzini, V., Stocker, D., and Bresch, D. N.: CLIMADA-project/climada_python: v3.0.1, https://doi.org/10.5281/zenodo.5555825, 2021.

Kropf, C. M., Ciullo, A., Otth, L., Meiler, S., Rana, A., Schmid, E., McCaughey, J. W., and Bresch, D. N.: Uncertainty and sensitivity analysis for probabilistic weather and climate risk modelling: an implementation in CLIMADA v.3.1.0 Non-peer reviewed preprint submitted to EarthArXi, EarthArXi, https://doi.org/https://doi.org/10.31223/X5GS7B, 2022.

Kyburz, M., Sovilla, B., Gaume, J., and Ancey, C.: Avalanche pressures at the Vallée de la Sionne test site: interaction of avalanches and narrow structures studied withe DEM, In International snow science workshop proceedings, pp. pp. 40–42, https://arc.lib.montana.edu/snow-science/item/2482, 2018.

Maggioni, M. and Gruber, U.: The influence of topographic parameters on avalanche release dimension and frequency, Cold Regions Science and Technology, 37, 407–419, https://doi.org/https://doi.org/10.1016/S0165-232X(03)00080-6, iSSW 2002: International Snow Science Workshop, 2003.

https://doi.org/10.5194/nhess-2022-112
Preprint. Discussion started: 6 April 2022


Natural Hazards and Earth System Sciences Discussions

Maggioni, M., Bovet, E., Freppaz, M., Segor, V., and Bühler, Y.: Potential of automated avalanche dynamic simulations for large scale hazard indication mapping in italy Potential of automated avalanche dynamic simulations for large scale hazard indication mapping in ital, International Snow Science Workshop ISSW, Innsbruck, Austria, 2018.

Mani, P. and Caduff, U.: Klimasensitivität Naturgefahren Teil 1 und Teil 2: Methodenbericht und Ergebnisse , Geo7 Bern, Tech. rep., Geo7, 2012.

Margreth, S.: Defense structures in avalanche starting zones. Technical guideline as an aid to enforcement Environment in Practice no. 0704, Tech. rep., Federal Office for the Environment, Bern; WSL Swiss Federal Institute for Snow and Avalanche Research SLF, Davos., https://www.slf.ch/fileadmin/user_upload/SLF/Permafrost/Bauen_im_Permafrost/Lawinenverbau_im_Anbruchgebiet_E.pdf, 2007.

Margreth, S., Burkard, A., and Buri, H.: Beurteilung der Wirkung von Schutzmassnahmen gegen Naturgefahren als Grundlagefür ihre Berücksichtigung in der Raumplanung, Tech. rep., Platform Naturgefahren PLANAT, https://www.gra-nat.ch/system/media/1800/original/PLANAT_2008_-_Teil_B__Lawinen.pdf?1421155223, 2008.

MATRIX Consortium: F. Wenzel, S. Laskowski and A. Garcia-Aristizabal, W. Aspinall and M. Bengoubou-Valerius, D. Monfort-Climent and N. Desramaut, A. Di Ruocco and K. Fleming, P. Gasparini and P. Gehl, B. Khazai and N. Komendantova, Z. Liu and J. Marti, W. Marzocchi and A. Mignan, R. Mrzyglocki and Nadim, F. and S. Parolai, A. Patt and A. Réveillère, A. Scolobig and S. Tyagunov, P. van Gelder and B. Vidar Vangelsten, C. Vinchon and S. Vorogushyn, J. Wang. MATRIX: New Multi-Hazard and Multi-Risk Assessment Methods for Europe, Tech. rep., Results I and Reference Report / Deliverable D8.4, https://cordis.europa.eu/project/id/265138/reporting, 2013.

MeteoSchweiz: Klimabulletin Jahr 2018, Tech. rep., Federal Office of Meteorology and Climatology MeteoSwiss, https://www.meteoschweiz.admin.ch/content/dam/meteoswiss/de/service-und-publikationen/Publikationen/doc/2019_ANN_d.pdf, 2019.

Monti, F., Alberti, R., Comin, P., Wolynski, A., and Bühler, Y.: Automated identification of forest with protective function against snow avalanches in the Trento Province (Italy), International Snow Science Workshop ISSW, Innsbruck, Austria, https://arc.lib.montana.edu/snow-science/item/2636, 2018.

Otth, L., Rüegsegger, C., Kropf, C. M., Ciullo, A., Meiler, S., Bresch, D. N., and McCaughey, J. W.: Analyzing Uncertainties in Climate Risk Assessment and Adaptation Options Appraisal with a Four-Phase Analytical Framework,, 2022.

Pancevski, B.: Snowbound Europe Struggles to Dig Out After Deadly Storms, The Wall Street Journal, 2019.

PLANAT: Risikokonzept Leitfaden Teil I Allgemeine Darstellung des Risikokonzepts und Teil II Anwendung des Risikokonzepts, Nationale Plattform Naturgefahren - Bründl M., Romang H., Holthausen N., Merz H., Bischof N., https://www.planat.ch/de/infomaterial-detail/risikokonzept-fuer-naturgefahren, 2009.

PLANAT: Umgang mit Risiken ausNaturgefahren. Strategie 2018., Tech. rep., Strategie 2018. NationalePlattform Naturgefahren PLANAT, Bern., https://www.newsd.admin.ch/newsd/message/attachments/53006.pdf, 2018.

Renner, K. and Steger, S.: Green Risk 4 Alps: WP3 Report on Results of the risk analysis and the strategyprioritization, Tech. rep., Interreg Alpine Space, 2021.

Rudolf-Miklau, F., Sauermoser, S., and Mears, A.: The Technical Avalanche Protection Handbook, Wiley-VCH Berlin, Germany, 430 pp.,, https://www.ernst-und-sohn.de/sites/default/files/uploads/media/sonderhefte/Technical_Avalanche_Protection_Detail_dt.pdf, 2014.

Salm, B., Burkhard, A., and Gubler, H. U.: Berechnung von Fliesslawinen., Eine Anleitung für den Praktiker mit Beispielen, Eidgenössisches Institut für Schnee- und Lawinenforschung SLF Davos, 1990.

Saltelli, A.: Sensitivity Analysis for Importance Assessment, Risk Analysis, 22, 579–590, https://doi.org/https://doi.org/10.1111/0272-4332.00040, 2002.

https://doi.org/10.5194/nhess-2022-112
Preprint. Discussion started: 6 April 2022


Saltelli, A., Aleksankina, K., Becker, W., Fennell, P., Ferretti, F., Holst, N., Li, S., and Wu, Q.: Why so many published sensitivity analyses are false: A systematic review of sensitivity analysis practices, Environmental Modelling & Software, 114, 29–39, https://doi.org/https://doi.org/10.1016/j.envsoft.2019.01.012, 2019.

Schneebeli, M. and Bebi, P.: HYDROLOGY | Snow and Avalanche Control, in: Encyclopedia of Forest Sciences, edited by Burley, J., pp. 397–402, Elsevier, Oxford, https://doi.org/https://doi.org/10.1016/B0-12-145160-7/00271-4, 2004.

Sovilla, B., Schaer, M., Kern, M., and Bartelt, P.: Impact pressures and flow regimes in dense snow avalanches observed at the Vallée de la Sionne test site, Journal of Geophysical Research: Earth Surface, 113, https://doi.org/https://doi.org/10.1029/2006JF000688, 2008a.

Sovilla, B., Schaer, M., and Rammer, L.: Measurements and analysis of full-scale avalanche impact pressure at the Vallée de la Sionne test site, Cold Regions Science and Technology, 51, 122–137, https://doi.org/10.1016/j.coldregions.2007.05.006, cited By 38, 2008b.

Teich, M., Marty, C., Gollut, C., Grêt-Regamey, A., and Bebi, P.: Snow and weather conditions associated with avalanche releases in forests: Rare situations with decreasing trends during the last 41 years, Cold Regions Science and Technology, 83-84, 77–88, https://doi.org/10.1016/j.coldregions.2012.06.007, 2012.

Trachsel, J.and Zweifel, B., Techel, F., and Marty, C.and Stucki, T.: Schnee und Lawinen in den Schweizer Alpen. Hydrologisches Jahr 2019/20, Tech. rep., WSL Institut für Schnee und Lawinenforschung SLF, https://www.wsl.ch/de/publikationen/default-a0030f2223.html, 2020.

van Westen, C. and Greiving, S.: Multi-hazard risk assessment and decision making, pp. 31–94, IWA Publishing, United Kingdom, https://research.utwente.nl/en/publications/multi-hazard-risk-assessment-and-decision-making, 2017.

Veitinger, J., Purves, R. S., and Sovilla, B.: Potential slab avalanche release area identification from estimated winter terrain: a multi-scale, fuzzy logic approach, Natural Hazards and Earth System Sciences, 16, 2211–2225, https://doi.org/10.5194/nhess-16-2211-2016, 2016.

Voellmy, A.: Über die Zerstörungskraft von Lawinen, Schweizerische Bauzeitung 73, 159–165, 1955.

Weber, D., Rüetschi, M., Small, D., and Ginzler, C.: Grossflächige Klassifikation von Gebüschwald mit Fernerkundungsdaten, Schweizerische Zeitschrift fur Forstwesen, 171, 51–59, https://doi.org/10.3188/szf.2020.0051, 2020.

Wiesinger, T. and Adams, M.: Schnee und Lawinen in den Schweizer Alpen. Winter 1998/1999, Tech. rep., SLF. Davos, Eidg. Institut für Schnee-und Lawinenforschung SLF., 2007.

ZAMG: Chimani, B. Ganekind M., Hiebl, J. Höfler A., Orlik, A. Österreichisches Klimabulletin Jahr 2019, Tech. rep., Zentralanstalt für Meteorologie und Geodynamik, https://www.zamg.ac.at/zamgWeb/klima/bulletin/2019/bulletin-2019.pdf, 2020.

Zgheib, T., Giacona, F., Granet-Abisset, A.-M., Morin, S., and Eckert, N.: One and a half century of avalanche risk to settlements in the upper Maurienne valley inferred from land cover and socio-environmental changes., Global Environmental Change, 65, 102 149, https://www.sciencedirect.com/science/article/pii/S0959378020307329, 2020.

Zweifel, B., Lucas, C., Hafner, E.and Techel, F., and Marty, C.and Stucki, T.: Schnee und Lawinen in den Schweizer Alpen. Hydrologisches Jahr 2018/19, Tech. rep., WSL Institut für Schnee und Lawinenforschung SLF, https://www.slf.ch/de/publikationen/default-34cd5573e3.html, 2019.